DEVELOPMENT OF SELF-DEGRADING 3D PRINTED POLYMER MATRIX COMPOSITES VIA MOISTURE ABSORPTION EVALUATION

by

Adedotun Banjo Dominic

A thesis submitted to the Graduate Faculty of
Auburn University
in partial fulfillment of the
requirements for the Degree of
Master of Science

Auburn, Alabama
August 8, 2020

3D-Printing, Polymer, Composites, Degradation, Moisture, Absorption

Approved by

Dr Asha-Dee Celestine, Chair, Assistant Professor Aerospace Engineering Department
Dr Vinamra Agrawal, Assistant Professor Aerospace Engineering
Dr Maria Auad, Professor Chemical Engineering Department

Abstract

Polymer degradation is a change in properties such as strength, color, shape, of a polymer or polymer-based material due to the effect of one or more environmental factors. These factors include heat, light or chemicals such as acids, alkalis and some salts. Polymer matrix composites exposed to moisture and high temperature environments can also experience several forms of degradation. Understanding how these composites degrade can help to develop degradable composites with the ability to self-degrade within a certain period of time. In this work, nylon, onyx (nylon reinforced with chopped carbon fiber) and polylactic acid (PLA) specimens were printed using a Markforged Mark Two and Maker Select v2 3D printers. The specimens were immersed in deionized (DI) water at 21^0C and 70^0C for different periods and characterized via moisture absorption and flexural testing. As expected, specimens exposed to higher temperatures displayed higher moisture absorption rates compared to specimens exposed to moisture at ambient temperature. Injection molded Nylon and PLA specimens were also tested and they displayed lower absorption rates compared to the 3D printed specimens. The specimens exhibited significant reduction in flexural strength and flexural modulus according to length of time immersed. Further characterization methods such as dynamic mechanical analysis (DMA), Fourier Transform Infrared Spectroscopy (FTIR), Differential Scanning Calorimetry (DSC) were also used. The factors investigated such as type of material, method of material production, absorption and desorption rates at different temperatures can be used as indices to develop degradation laws for polymer matrix composites.

Acknowledgments

I give all the Glory to God my father in Heaven - the Most High who ruleth in the kingdom of men. I am forever grateful to my academic advisor Dr Asha-Dee Celestine, who was an integral part of this project. I am thankful to her for her professional guidance and mentorship. I am also grateful to my committee members Dr Maria Auad and Dr Vinamra Agrawal. Dr Auad gave me a strong foundation in this field of research and her wealth of experience was immeasurably helpful in this work. Dr Agrawal's area of aeromechanics helped me to understand the mechanics of this research work. And to Dr Ramsis Farag who always made his lab available for me to come in and work, his tutelage and willingness to assist me on the equipment every time helped me immensely in this work. To my parents whose prayers and support has brought me thus far in life – thank you so much. I am also grateful to all my brothers and sisters for their love and support over the years. And finally to all my friends, you guys are the best.

Table of Contents

List of Tables

List of Figures

List of Abbreviations

3DP	3D Printed
IM	Injection molded
PLA	Polylactic acid
FDM	Fused Deposition Modelling
DI	Deionized
FTIR	Fourier Transform Infrared Spectroscopy
DMA	Dynamic Mechanical Analysis
DSC	Differential Scanning Calorimetry

1.0 INTRODUCTION

1.1 Degradation in Polymer Matrix Composites

Polymer degradation is a change in properties which may be strength, color, shape, or any other property of a polymer or polymer-based material due to the effect of one or more environmental factors. These factors include heat, light or chemicals such as acids, alkalis and some salts [1]. When a material degrades, it may lead to the destruction of a part, and in extreme cases loss of life and property. As a result, these unwanted circumstances must be avoided. Material structure, as well as exposure conditions are some of the major factors responsible for polymer material degradation. Physical polymer degradation may be caused by the disruption of the polymer morphology, environmental stress cracking or thermal embrittlement [1]. Polymer matrix composites (PMCs) are composed of a several continuous or short fibers bound together by an organic polymer matrix. When exposed to moisture and high temperature environments PMCs can experience several forms of degradation. Understanding how these composites degrade can help to develop degradable composites with the ability to self-degrade within a certain period of time. Figure 1.1 highlights some of the factors that may cause degradation of a material and the type of degradation that results from the effects of such factors.

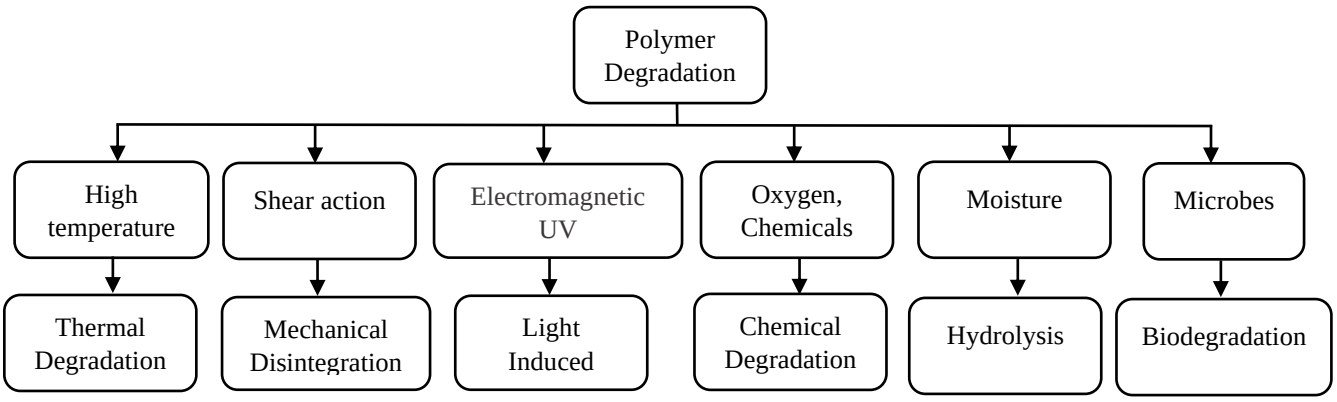

Figure 1. 1 Factors which may cause polymer degradation in relation to the type of degradation.

As illustrated in the various degradation scenarios, a combination of these stimuli is usually observed. The current study focuses on thermal and moisture-induced degradation. Moisture absorption in PMCs at ambient temperature and elevated temperature occurs at various rates which may lead to changes in its thermal and mechanical properties [2]. Factors responsible for the moisture absorption behavior of polymers include microstructure and molecular structure, as well the degree of crosslinking, the polarity of molecular structure and the presence of residual monomers [1-2].

1.2 Moisture absorption in polymers

Moisture absorption plays a significant role in the properties of a material. However, the ability and extent to which a material may absorb moisture is dependent on factors such as the surrounding temperature, humidity and the length of time the material has been exposed to the environment. Many authors have studied this phenomenon for several years [3-5,6-8].

In general, moisture penetration into polymers occurs via diffusion of water molecules through the material [9-11]. Here, water is transported to the interior of the polymers due to random molecular motions and the rate at which this occurs depends strongly on temperature and ambient relative humidity. As moisture diffuses into the polymer it leads to changes in both mechanical and thermophysical properties [12,13]. At the microscopic level, the moisture diffusion behavior of polymers depends on polarity, degree of crosslinking, and the presence of residual monomers, hardeners, or other water attracting species [14,15]. Moisture absorption may be measured as the increase in mass after exposure to wet environments [3-5]. In 1856, Adolf Fick derived the Fick's law of diffusion which is used today to model the moisture diffusion and total water absorbed in polymers and polymer matrix composites. The classical Fickian absorption mechanism postulates that weight gain (percentage) as a function of square root of time at the early stages of diffusion is

linear. At longer periods, the curve steers downwards towards the horizontal axis, and at much longer periods the curve attains a final equilibrium value where the material is fully saturated [5].

There are, however, instances in hygrothermal aging where significant deviations from the Fickian diffusion laws have been observed [3,4]. These non-Fickian behavior studies reveal that diffusion may be affected by rate of absorption through voids and microcracks, capillary actions (wicking) or via percolation of the matrix. [16]. At elevated temperatures and elongated periods, faster absorption rates are observed. This observation can be explained by the fact that diffusion is a temperature-dependent phenomenon. Figure 1.2 highlights the different behavioral patterns of water absorption and desorption in polymers and polymer composites. The curves A, B, C and D represents the non-Fickian weight-gain sorption, weight gain versus $M(t^*)/M(\infty)$ versus $\sqrt{t^*}$ where $t^* = \frac{Dt}{L^2}$, M is moisture, D is the diffusion coefficient, t^* is the period and L is the length of the specimen [4]. *LF* is the Linear Fickian diffusion. Curve A represents a steady increase in weight gain, which never reaches an equilibrium, while curve B denotes a so-called two stage diffusion pattern. The progression in the curves *A* and *B* occurs due to two competing absorption rates via water diffusion and polymer relaxation [17]. Curve C represents a rapidly increasing moisture content within the polymer followed by damage increase, mechanical failure and large deformations. In curve D weight loss due to irreversible physical/chemical breakdown is illustrated. In many situations, weight loss is a function of hydrolysis which is the separation of side groups from the polymeric chains and possible chain breakdown, or the dissociation of matter located [15]. Some common polymers which undergo hydrolysis after moisture absorption are nylon and polylactic acid (PLA).

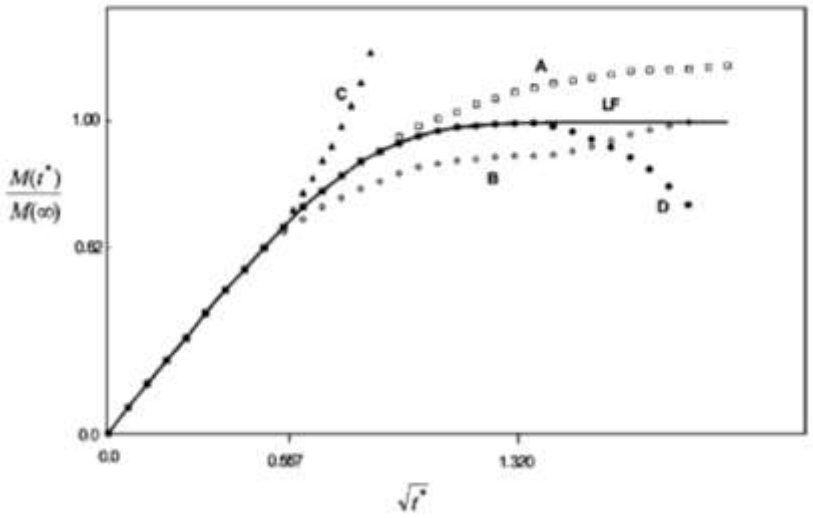

Figure 1. 2 Schematic curves showing the plots for four kinds of recorded non-Fickian weight gain sorption [15].

1.3 Moisture Absorption in Nylon

Nylons is a thermoplastic polymer well known for its hygroscopicity – that is, it readily absorbs moisture from the environment [18]. At elevated temperatures, and in the presence of moisture, nylon also has the potential to degrade via the hydrolysis of the amide linkages in its backbone which often leads to the dissociation of the amide bonds and shorter chains, as well as lower molecular weight [19,20]. Consequently, significant reductions in both mechanical and thermal properties are observed after exposure to wet environments. Figure 1.3 illustrates the hydrolysis of nylon in the presence of moisture and heat.

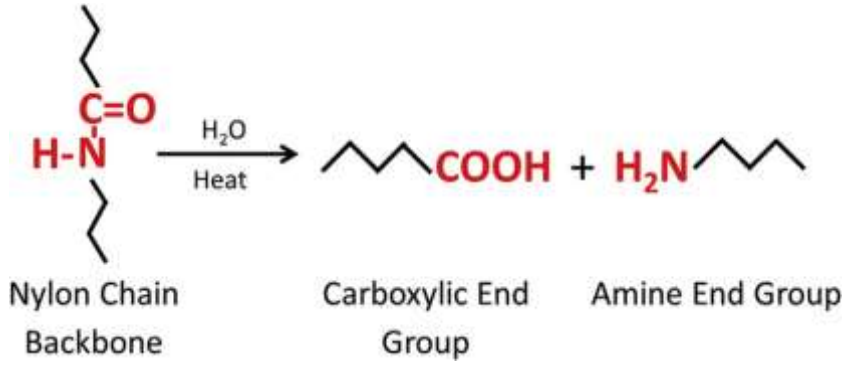

Figure 1. 3 Mechanism of hydrolysis of nylon in the presence of heat and moisture [21].

Water molecules are broken up into hydrogen (H^+) and hydroxide (OH^-) ions, which further reacts with and breaks the amide bond in the presence of heat [22]. Therefore, a critical measure to prevent hydrolysis nylon is to first dry the material before processing [21]. Nylon also suffers a reduction in its durability due to the plasticization of the chains and, in the case of composites, debonding of the filler-matrix interface via swelling and weakening of the phase boundary [23-24]. Moisture in nylon functions as a plasticizer and is responsible for the reduction in the entanglements and subsequent bonding between the molecules, resulting in reduced glass transition temperature, T_g [25]. At short periods of immersion in water at elevated temperatures, nylon may exhibit enhanced ductility due to the increased moisture absorbed, but also suffers from reduced strength and modulus.

1.4 Moisture Absorption in PLA (Polylactic acid)

Polylactic acid (PLA) is a thermoplastic aliphatic polyester derived from renewable resources. It is widely used in biomedical and industrial applications as a material for tissue engineering or in the preparation of bio-plastic products such as food packaging or disposable tableware [26]. PLA is obtained from pure L-lactic and D-lactic isomers, which leads to poly-L-lactic (PLLA) acid and poly-D-lactic acid (PDLA) homopolymers, respectively [27].

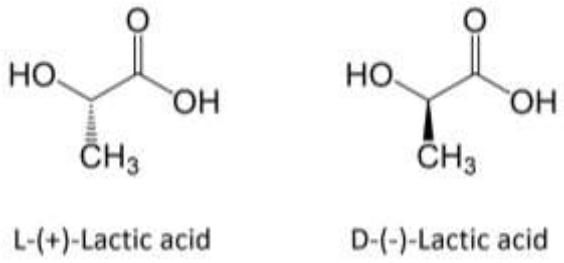

Figure 1. 4 Lactic acid enantiometers [26]

The presence of polar oxygen linkages in PLA makes it a naturally occurring hydrophilic polymer. However, due to the existence of methyl side groups, PLA is also hydrophobic [28].

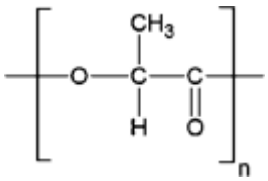

Figure 1. 5 Atomic chemical structure of polylactic acid (PLA) [29]

The interplay of these hydrophobic and hydrophilic properties is largely responsible for its moisture absorption kinetics and consequent degradation behavior. PLA degrades under hydrolytic conditions leading to significant reductions in molecular weight and mechanical properties [30,31]. During hydrolysis of PLA, the ester bonds are broken down by the water molecules, resulting in the reduction of the molecular weight to values below 10 kDa even before it becomes degradable [31]. Early studies have revealed that PLA is fairly stable in water at mesophilic temperatures (15^0C-40^0C) where it has the capacity to absorb between 0.7 -1% of water in 30 days [32] or slightly more at longer periods of immersion [33]. According to Yew et al., both the matrix polymer and its biocomposites were affected by hydrothermal ageing. In their work rice starch (20%)/PLA biocomposites were aged in water at 30^0C for 30 days. The PLA tensile modulus reduced from 3.3GPa to 2.9GPa, its yield strength from 58MPa to 54MPa, while the strain at failure dropped from 3.8% to 3.2.%. These results were attributed to the changes in the properties of PLA due to hydrolysis after the immersion.

1.5 Additive Manufacturing

About 36 years ago, Charles W. Hull pioneered a revolutionary idea to build objects by Additive Manufacturing (AM) or 3D printing technology [34-36]. Additive manufacturing technology is a novel technique that creates objects through digitized models without traditional cutting or casting machines which can be expensive [37-41]. AM also has tremendous advantage of producing parts with intricate shapes and out of multi-materials components, which other methods cannot do [34,42–45]. Today, this technology has traversed several fields such as

biomedicine, aerospace, automotive engineering, civil engineering and the food industry [46-53]. 3D printing offers tremendous advantages in the manufacturing industry and may even replace injection molded methods where melt lines and weld lines design restrictions, and high initial tooling cost are major manufacturing issues [54].

Fused Deposition Modeling (FDM) was introduced in the early 1980's and has remained arguably the most common method of Additive Manufacturing method used to fabricate polymer and polymer matrix composites components [55]. In this 3D printing method, the thermoplastic is melted and extruded via a heated nozzle that deposits layers upon layers on a platform print (bed) to build the object [56]. Most common filaments available today include nylon, PLA and acrylonitrilebutadiene styrene (ABS). FDM has remained in the market for over two decades due to material availability, low cost and less processing.

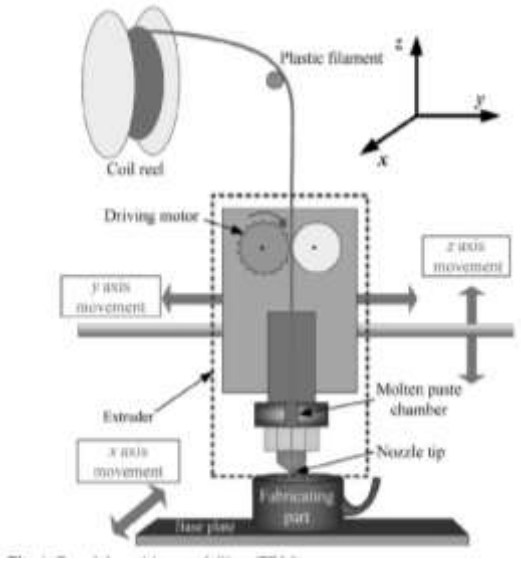

Figure 1. 6 Schematic of Fused Deposition Modelling [57].

In 3D printed polymer materials, moisture can meander through the pores and the layers which can initiate degradation after a long period of exposure. The objective of this work was to evaluate and compare the change in properties of 3D printed nylon, 3D printed Onyx, 3D printed PLA and injection molded nylon due to the moisture absorption. The effect of immersion time and

temperature on the moisture absorption rate and the flexural and thermomechanical properties of these materials was investigated. 3D printed nylon and 3D printed PLA were evaluated to examine the effect of the hygroscopic nature of the polymer on the change in properties since nylon and PLA have different absorption and desorption rates. By comparing 3D printed and injection molded nylon, this work also sought to investigate the effect of fabrication technique on moisture absorption and change in properties. The 3D printed specimens would have a layered nature which should affect their moisture absorption characteristics. Tests such as dynamic mechanical analysis (DMA), Fourier transform infrared spectroscopy (FTIR), and differential scanning calorimetry (DSC) were also performed to further evaluate and understand the degradation kinetics of these materials.

2.0 EXPERIMENTAL PROCEDURE

The overall structure of the research work is outlined in Figure 2.1. The specimens were initially designed in SolidWorks, then 3D printed. After printing they were conditioned at 50^0C for 24 hours, followed by immersion in deionized (DI) water for several periods. After immersion they were characterized via moisture absorption analysis, flexural mechanical testing, DSC, FTIR and DMA.

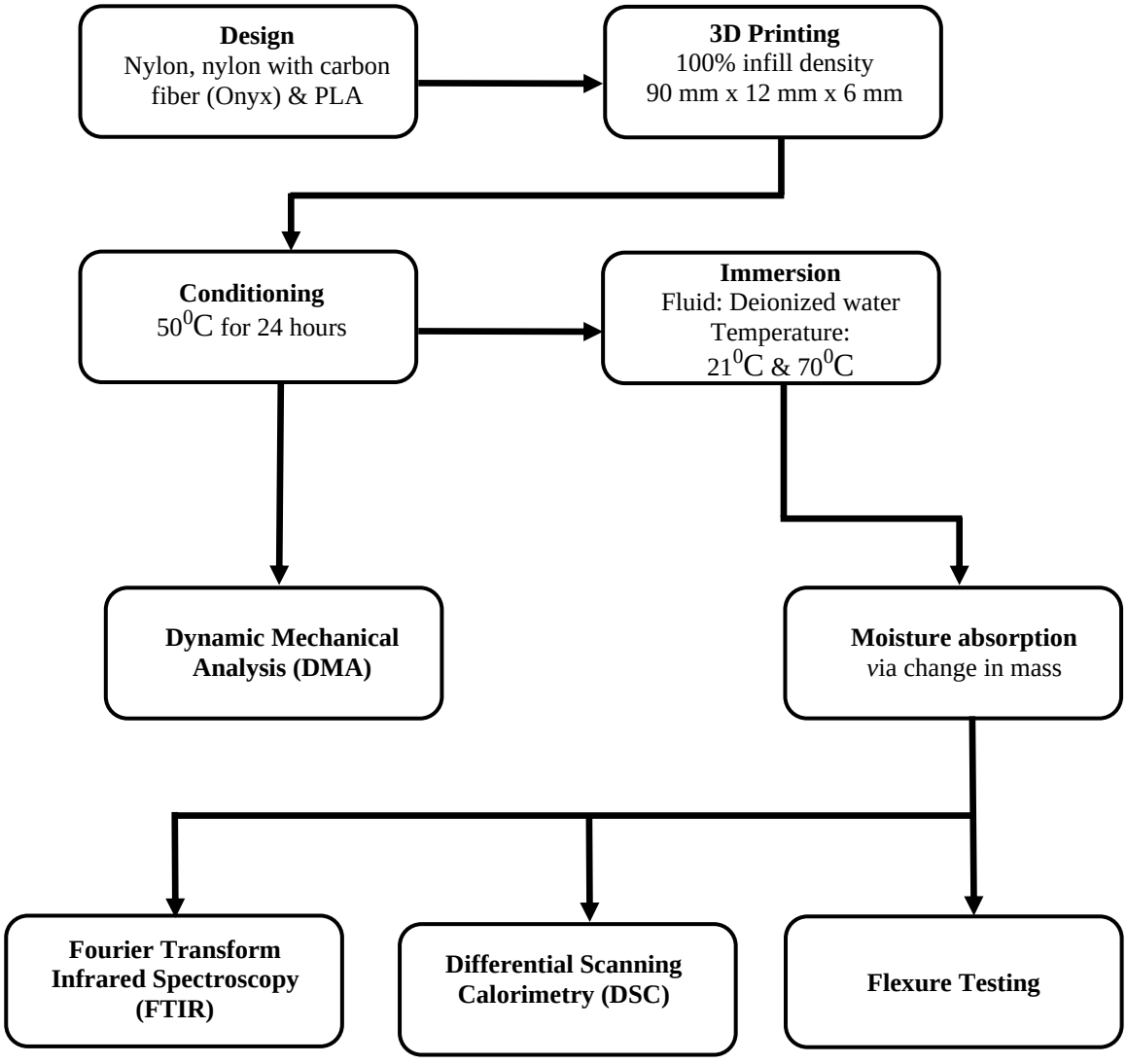

Figure 2. 1 Flowchart of experimental procedures followed.

2.1 Materials and Methods

2.1.1 Materials

The materials used in this research were fabricated via 3D printing on the Markforged and Maker Select v2 3D printers. Nylon, Onyx (nylon reinforced with chopped carbon fibers) and PLA specimens were printed. Markforged's 1.75mm 3D printing filaments were used for the nylon and Onyx specimens while the Hatchbox brand of filaments (1.75mm) was used for the PLA specimens. The specimens were first designed in SolidWorks with dimensions 90mm x 12mm x 6mm for flexure testing. Specimens for DMA and moisture absorption analysis were dimensioned 30mm x 10mm x 3mm. Injection molded nylon specimens with dimensions 120mm x 12mm x 3mm were obtained from Plasticomp Inc. Schematics of each specimen type are shown in Figure 2.2 and their dimensions are summarized in Table 2.1. Print parameters are summarized in Table 2.2.

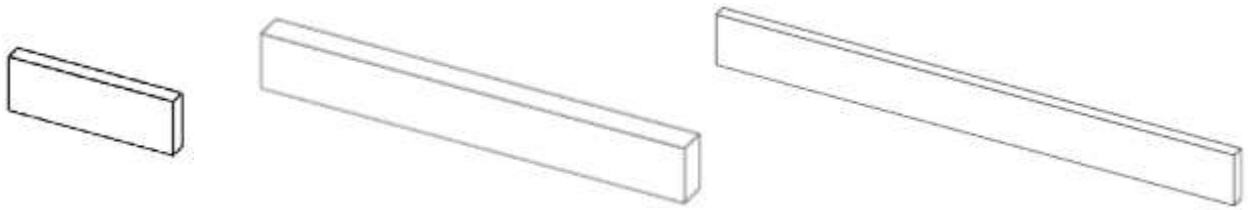

Figure 2. 2 Schematic of specimens used (a) Dynamic Mechanical Analysis (b) 3D printed flexure and (c) Injection molded flexure specimens.

Table 2. 1 Dimensions of specimens

Specimen Type	Length (mm)	Width (mm)	Thickness (mm)
DMA	30	10	3
Flexure – 3D printed	90	12	3
Flexure - Injection molded	120	12	6

Table 2. 2 Printing parameters for FDM process

Printer model	Maker Select v2 3D Printer	Markforged Mark Two
Cooling fan speed	100%	N/A
Filament diameter	1.75mm	1.75mm
Bed temperature	60^0C	N/A
Layer height	0.1 – 0.3mm	0.1mm
Printing temperature	220^0C	275^0C
Infill pattern rectilinear	±45	±45
Infill density	100%	100%
Slicer software	Cura	Eiger

(a) **(b)**

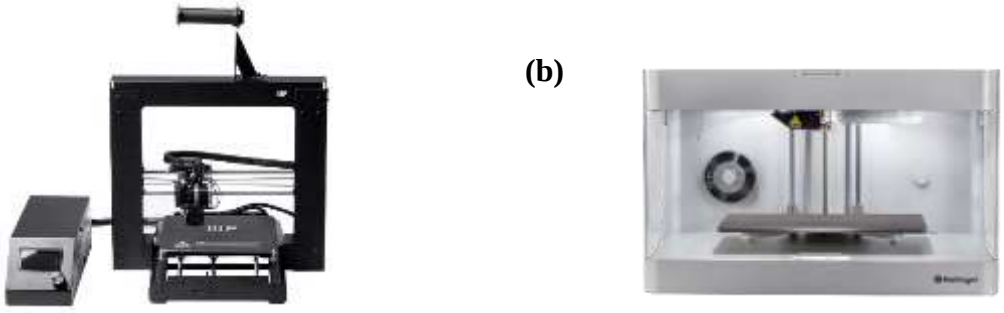

Figure 2. 3 3D printers used (a) Maker Select v2 3D Printer (b) Markforged Mark Two 3D Printer.

2.1.2 Methods

All specimens were conditioned in the oven at 50^0C for 24 hours to remove any surface moisture which may be present. Specimen mass was recorded before and after conditioning. Specimens were then soaked in deionized (DI) water for increasing periods at ambient temperature of 21^0C, and at elevated temperature of 70^0C to evaluate the effect of moisture and temperature on material properties. Several tests were performed to characterize material behavior, including Fourier Transform Infrared Spectroscopy (FTIR), Dynamic Mechanical Analysis (DMA) and flexure testing. The material properties of the materials investigated, as reported by the manufacturers are shown in Table 2.3 [58].

Table 2. 3 Material properties for 3D printed nylon, 3D printed onyx, Injection molded nylon and 3D printed PLA [58-60].

Property	Test Standard	3DP Nylon	3DP Onyx	IM Nylon	3DP PLA
Tensile Strength (MPa)	ASTM D638	54	36	61.8	37
Tensile Modulus (GPa)	ASTM D638	0.94	1.4	2.5	3.5
Tensile Strain at Break (%)	ASTM D638	260	58	60	6
Flexural Strength (MPa)	ASTM D790	32	81	123	103
Flexural Modulus (GPa)	ASTM D790	0.84	2.9	2.4	4
Flexural Strain at Break (%)	ASTM D790	N/A	N/A	N/A	N/A
Heat Deflection Temp. (^{0}C)	ASTM D648	44-50	145	57	52
Density (g/cm^3)		1.10	1.18	1.14	1.3

2.2 Moisture Absorption

Moisture absorption was carried out according to ASTM standards D570 [61]. After conditioning, specimens with dimensions 30mm x 10mm x 3mm were immersed in deionized (DI) water at 21^{0}C and 70^{0}C. At various times, ranging from 30 minutes to 28 days, the specimens were removed, carefully dried with a paper towel and their mass recorded using a VWR analytical balance. Their change in mass was calculated using Equation 1

$$M(\%) = \frac{M_f - M_i}{M_i} \times 100 \quad (1)$$

where M is percentage moisture absorption, M_f is final mass (in grams) absorbed after time t, and M_i is the initial mass before immersion (in grams). Plots of percentage moisture absorption versus square root time were then generated for each material and temperature.

2.3 Dynamic Mechanical Analysis (DMA)

Moisture absorption and temperature effects will lead to the materials exhibiting changes in viscoelastic behaviors. This phenomenon was studied using dynamic mechanical analysis (DMA). A TA-RSA3 dynamic mechanical analyzer was used. According to ASTM D4065 [62], DMA was used to determine the glass transition temperature (T_g) and the storage modulus (E') of

each material before and after immersion. Specimens with dimensions 30mm x 10mm x 3mm were used and testing was performed with 25 mm support span and 0.1% maximum strain. Specimens were subjected to a temperature ramp of 25^0C to 100^0C, with a heating rate of 5^0C/min at a frequency of 1 Hz. The temperature at which the tan delta curve transitioned from the glassy state to the rubbery region was taken as the glass transition temperature (T_g), while the storage modulus, *E'*, was the *E'* value at ambient temperature.

2.4 Fourier-transform infrared spectroscopy (FTIR)

Fourier-transform infrared spectroscopy (FTIR) is a non-destructive testing technique that may be used to identify functional groups in a polymeric material. This test is carried out according to the ASTM D5477 standard [63]. This method is important in the study of polymer degradation as it can identify the chemical changes that have occurred in the microstructure of the material at it probes the interference of infrared light and chemical bonds [64]. The chemical bonds vibrate due to the impinging light waves (magnetic and electrical waves). As a result, light with specific wavenumbers can be absorbed or transmitted by the molecules. The measurement of these wavenumbers reveals the types of chemical bonds or functional groups present in the molecules as well as their estimated amount [62].

The 3DP nylon, 3DP onyx, injection molded nylon and 3DP PLA were studied via FTIR spectroscopy to identify the various functional groups present and to understand the degradation mechanisms after 14 days of immersion in DI water at 21^0C and 70^0C. A Thermo Scientific Nicolet 6700 spectroscope fitted with a CsI attenuated total reflection (ATR) detector was used for this investigation. FTIR spectra, in absorbance mode, were detected using a scanning resolution of $2cm^{-1}$ and 32 scans for each specimen in the range of $4000–400cm^{-1}$. Subsequent data analysis

was then performed on the resulting spectra to determine if any changes in microstructure had occurred.

2.5 Differential Scanning Calorimetry (DSC)

Differential Scanning Calorimetry (DSC) is a technique used to evaluate the thermal transitions of polymeric materials. It measures the enthalpy changes in the physical and chemical properties of a sample material as a function of time or temperature [10]. By measuring the amount of heat produced as a sample is heated or cooled, chemical reactions and thermal transitions such as glass transition, crystallization and melting temperatures can be identified. DSC analysis was conducted on the four materials before immersion and after 14 days of immersion in DI water. A DSC Q200 manufactured by TA Instruments was used. Heating and cooling rate, from 23^0C-260^0C, was 10^0C/min, according to ASTM Standard D7426 [65]. The results were then used to determine the melting temperature (T_m), crystallization enthalpy (ΔH_c) and melt enthalpy (ΔH_m) of each material. Percentage crystallinity was calculated using Equation 2, where ΔH_m and ΔH_c are the melting and cooling enthalpies for 100% crystalline material. Note that theoretical enthalpies of melt (ΔH_m) for nylon and PLA are 230.1J/g [66,67] and 93J/g [68] respectively.

$$\% \text{ Crystallinity } (X_c) = \frac{\Delta \mathrm{H}m}{\Delta \mathrm{H}m100} \; X \; 100\% \tag{2}$$

2.6 Flexural Testing

3-point bend flexure testing was performed using an Instron mechanical test frame (Model 5565, 5 kN load cell) with a cross-head speed of 3 mm/min according to ASTM standard D7264 [69]. 3D printed specimens measured 90 x 12 x 6mm, while injection molded specimens measured 120 x 12 x 3mm. Specimens were soaked in DI water at 21^0C and 70^0C for varying time periods ranging from 12 hours to 28 days and then tested. Load and displacement data were collected every 0.02 seconds. The flexure stress (σ_f) and flexure strain (ε_f) were calculated using Equations 3 and

4 respectively. The flexural modulus was the slope of the linear region of stress versus strain plot over a range of 0.2% strain, while the yield strength was the corresponding stress value using a 0.2% strain offset.

$$\sigma_f = \frac{3PL}{2bh^2} \tag{3}$$

$$\varepsilon_f = \frac{6\delta h}{L^2} \tag{4}$$

where P denotes the flexure load (N), L is the support-span (mm), b is the specimen width (mm), h is the specimen height (mm) and δ is the maximum deflection of the beam (mm). The results were then used to evaluate the change in properties of the 3D printed, as well as injection molded specimens when exposed to hot, wet environments.

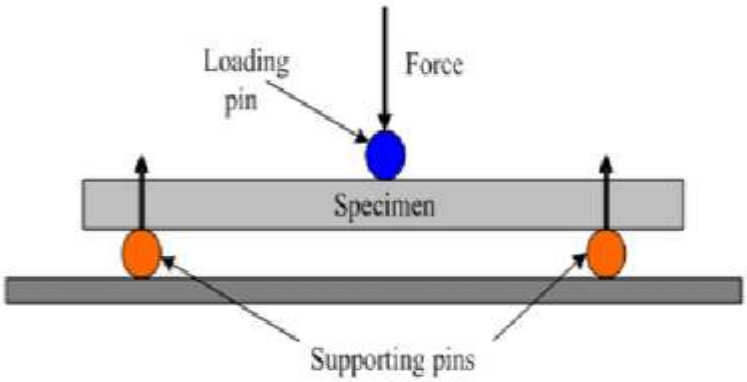

Figure 2. 4 3-point bent flexural test set up

3.0 MATERIAL CHARACTERIZATION

3.1 Moisture Absorption

Materials exposed to moisture either in hot or wet environment tend to absorb moisture. In the long run, this moisture absorption can lead to diffusion of the water molecules into the materials themselves and can have damaging effects on the mechanical and physical properties, and hence performance of the materials [70-72]. As a result, it is critical to correctly predict the life cycle of polymer composites and also design them based on their absorption and desorption mechanics. It is important to note that models such as the Fickian diffusion has been developed to describe the kinetics of moisture absorption in polymer matrix composites and even in the cases (non-fickian) of moisture absorption for thermosets [73-77]. These models ensure the determination of moisture concentration profiles and time-dependent weight gain all which can be used to study periodical changes and variations in the materials [78-80].

In this study, the absorption phenomena at the two different temperatures 21^0C and 70^0C were studied for four materials – 3DP nylon, 3DP Onyx, injection molded nylon and 3DP PLA. The pores between the layers of 3D printed materials served as moisture absorption inlets thus aiding rapid moisture uptake.

As illustrated in Figure 3.1, 3DP nylon soaked at ambient temperature experienced a linear rise in moisture absorption percentage up to a maximum of ~9.5% then reduces gradually desorbing down to ~6% at which this equilibrium is attained for as long as ~9 months. While at 70^0C maximum moisture was attained at ~7% followed by the onset of desorption down to ~2% after 14 days of immersion in DI water.

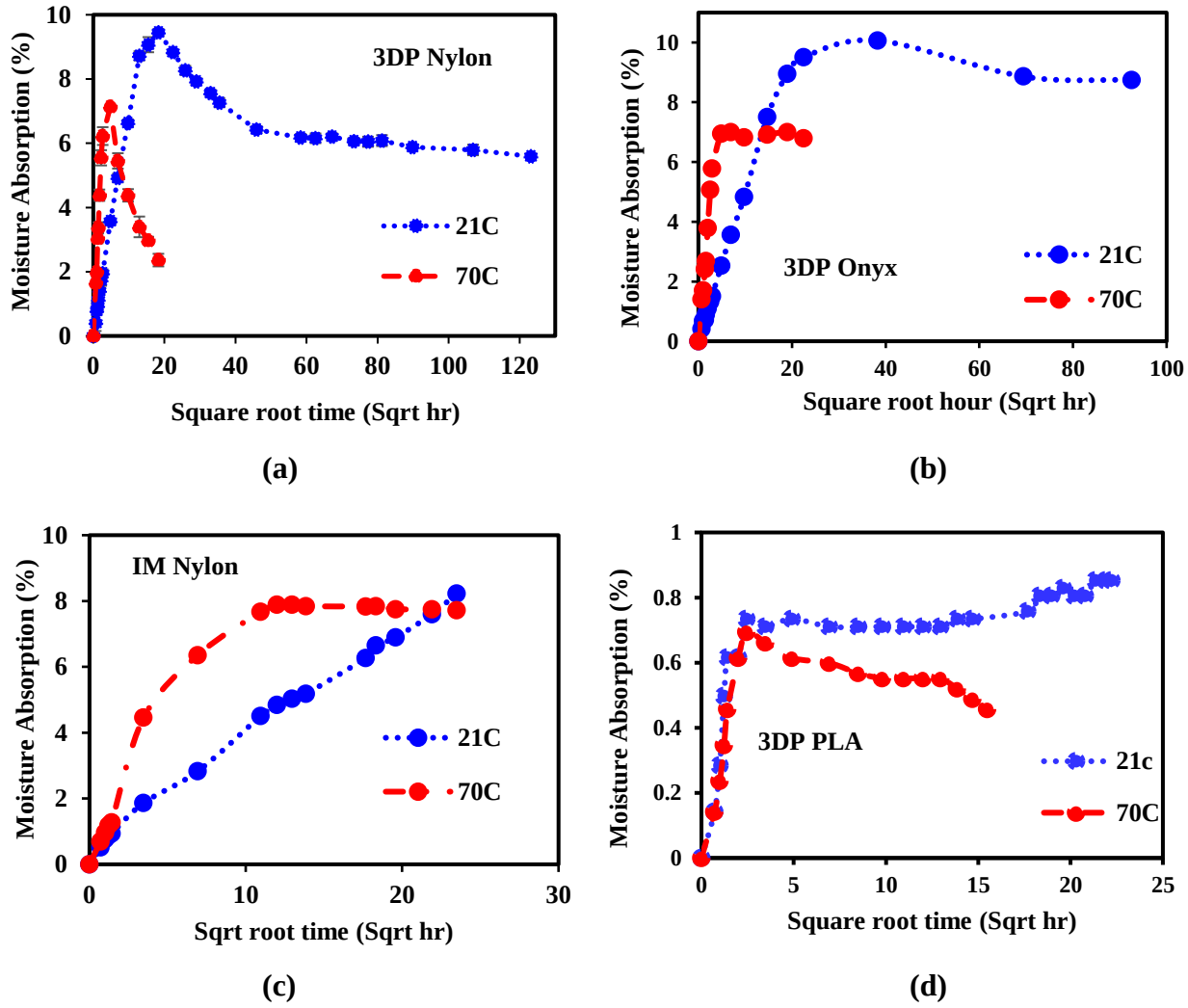

Figure 3. 1 Moisture absorption behavior of 3D printed materials after immersion (a) Nylon (b) Onyx (c) Injection molded nylon (d) PLA

In the 3DP Onyx material at ambient temperature, maximum moisture absorption is attained at ~10% before equilibrium was maintained for longer immersion times. The maximum percentage moisture absorbed is ~7% at 70^0C before equilibrium. IM nylon at both temperatures has a maximum at ~8%. It is important to note that conditions of elevated temperatures of 70^0C had earlier been responsible for the equilibrium attained at ~8% which is maintained for longer

periods before intersecting with the specimen soaked at 21^0C which is yet to attain equilibrium for the time period investigated.

3DP PLA exhibits very different moisture absorption behavior from the nylon and nylon matrix composite specimens. Maximum moisture absorption attained is ~1% for both temperatures. Specimens soaked at ambient temperature maintains this trend as an equilibrium, while specimens soaked at elevated temperature of 70^0C begins to desorb down to as low as ~0.5% after 10 days of immersion in DI water. The moisture absorption trends observed in this study were in close conformity to those presented by other researchers.

3.2 Dynamic Mechanical Analysis

Dynamic mechanical analysis (DMA) is a test used to study the viscoelastic behavior of materials. Here, the aim is to investigate and understand how the material behaves as the temperature changes. Parameters such as the glass transition temperature, the storage and loss modulus of the materials are indices used in the study [81]. The glass transition temperature, Tg is the temperature below which the physical properties of materials change to that of a glassy state possessing relative mobility, above T_g the material behaves like a rubbery material. The storage modulus E' and loss modulus E" in viscoelastic materials measure the stored energy (representing the elastic portion), and the energy dissipated as heat (representing the viscous portion), respectively [81]. Tan delta (*tan δ*) is the ratio of the storage modulus to the loss modulus, and can be interpreted as the midpoint between the glassy and rubbery states [81].

Table 3. 1 Storage modulus and glass transition temperature measurements for 3DP nylon, 3DP Onyx, IM nylon and before soaking.

Material	Storage Modulus E' (GPa)	Glass Transition Temperature T_g (C)
3DP nylon	1.04	36.1
IM nylon	2.3	40.0
3DP PLA	2.2	68.6

The glass transition of the virgin 3DP nylon is ~36.1^{0}C and this indicates that this is the range where the materials transitions from its crystalline state to the rubbery region. It is believed that at this region the polymer chains have gained a measure of mobility; where vibrations of the long molecular chains of the amorphous phase [21] region was used in determining the glass transition temperature of the 3DP nylon material. In like manner, IM nylon transitioned at ~40^{0}C while the storage modulus was 2.3GPa. Although both nylon materials contain the same molecules and bonds, the slight disparity is likely due to the difference in source of the nylon and the method of fabrication. The lower rigidity in the 3DP nylon accounts for the lower E' values against that obtained from the IM nylon. The 3DP PLA glass transition temperature was ~69^{0}C indicating that at this temperature the polymer chains have more mobility. It is important to mention that these values correspond to values obtained by other researchers. At the time of this publication virgin 3DP Onyx data was not obtained due to equipment limitations.

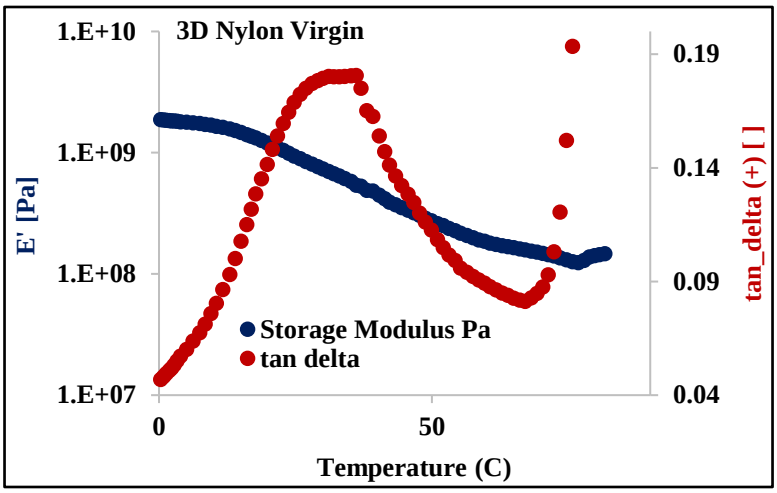

(a)

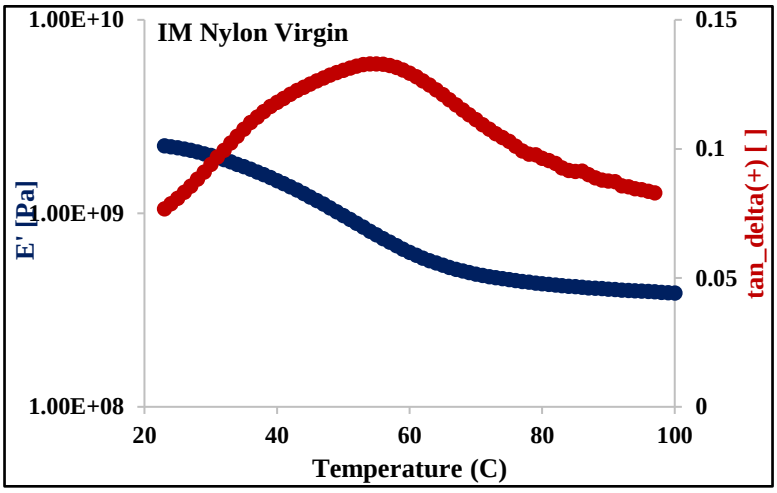

(b)

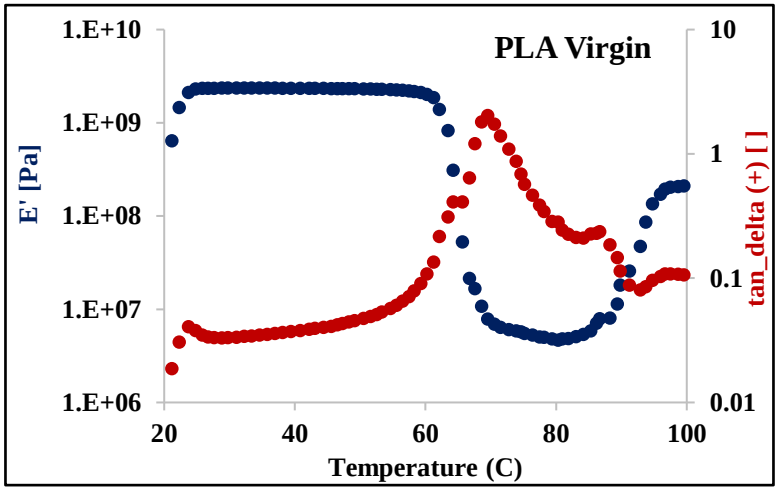

(c)

Figure 3. 2 Dynamic Mechanical Analysis of virgin materials before immersion in DI water (a) 3DP Nylon (b) Injection molded nylon (c) 3DP PLA

3.3 Fourier Transform Infrared Spectroscopy

IR spectroscopy was employed to identify the basic structural units present in the four materials 3DP nylon, 3DP Onyx, IM nylon and 3DP PLA. The results are shown in Figures 3.3 - 3.6. FTIR spectroscopy can be used to investigate changes in the polymer molecules as they degrade after immersion. Changes in the intensity of the signals regarding specific chemical groups is used for the analysis of the mechanism of molecular interaction.

3.3.1 IR analysis of 3DP Nylon

In the FTIR analysis spectra of virgin 3DP Nylon (Figure 3.3), the bands at 3320cm^{-1} and 3210 cm^{-1} represent the stretching and deforming N-H bonds respectively, while the bands at 1478cm^{-1} and 752cm^{-1} are the wagging vibrations of N–H bonds [21,82]. The bands at 3081cm^{-1} and 3020cm^{-1} are a function of the asymmetric and symmetric stretching vibrations of C–H bonds. The bands at 2968cm^{-1} and 2856cm^{-1} are due to the asymmetric and symmetric CH_2 stretching vibrations respectively. The C=O stretching vibrations is in the region 1732cm^{-1}, while 1663cm^{-1} gives the stretching (amide 1) NH band, 1542cm^{-1} the asymmetric deformation (amide II) band, and finally wagging of NH (amide III) band is observed at 1345cm^{-1} [82]. The bands found at around 1142cm^{-1} is the CO–CH symmetric bending vibration combined with CH_2 twisting. The bands at 931cm^{-1} and 610cm^{-1} are the stretching and bending vibrations of C–C bonds respectively, while the band at 591cm^{-1} is due to O=C–N bending [80]. As these materials were exposed to moisture at elongated periods (14 days), the water gradually diffused into the nylon matrix forming hydrogen bonds with the amide groups forming tightly and loosely joined bound water molecules [81-85]. While the loosely joined molecules form congregates around the tightly joined molecules and can be removed easily via heating, the tightly joined molecules are the main polymer chains attached to the amide groups of the nylon. Spacing in the nylon polymer is due to the presence of

these congregates which leads to the eventual swelling of the nylon polymer in the presence of water and which is rapid at elevated temperatures [21]. The IR results obtained after 14 days of immersion in water at 21^0C and 70^0C illustrate the effects of water on the nylon specimens and eventual structural changes. In the Figure 3.3 the shifts and different peak intensities at 21^0C and 70^0C are readily noticeable and are due to the effects of the absorbed water. It is noteworthy that the presence of peaks at 1471cm^{-1},1460cm^{-1} and 1420cm^{-1} can be attributed to the CH_2 scission bending of the vibrations of the α, γ, α-phases respectively [86]. The nylon polymer chains are closely packed in the α-phase region, thus constricted vibrations of the CH_2 groups whereas the γ-phase has more molecular chain movements due to less constrictions. At elongated periods, the moisture gradually begins to push the nylon polymer chains apart creating empty spaces allowing for more bending vibrations of the CH_2 groups [80]. These structural changes will also lead to changes on both the glass transition temperature and crystallinity, as will be shown in the DSC analysis. At 21^0C, hydrolysis is not as significant compared to the response at 70^0C. Higher temperatures lead to faster rate of hydrolysis, then the crystalline phase experiences more permeation, suggesting greater dissociation.

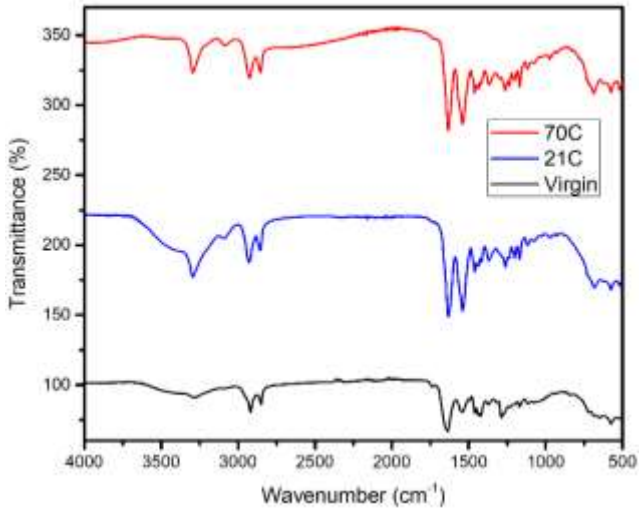

Figure 3. 3 FTIR plot for 3DP nylon specimen before and after immersion in DI water for 14 days.

3.3.2 IR analysis of 3DP Onyx

While the FTIR analysis spectra of the onyx sample (Figure 3.4) is not much different from nylon, the peaks are located at slightly different wave numbers. This is expected as onyx is a carbon reinforced nylon composite. After 14 days, peaks at 1669cm^{-1} and 1535cm^{-1} show increased intensities of the amide I and II groups respectively. Further changes are observed after immersion, especially at elevated temperatures of 70^{0}C. The bands found at circa 1154cm^{-1} are the CO–CH symmetric bending vibration and CH_2 twisting, while the bands at 920cm^{-1} and 620cm^{-1} are the stretching and bending vibrations of C–C bonds. Lastly, the band at 580cm^{-1} is due to O=C–N bending. Even at elevated temperatures and longer periods of immersion, however, scission is limited compared to the IM nylon and 3DP nylon. This result is possibly due to the carbon reinforcement in the nylon matrix that limits the formation of hydrogen bonds.

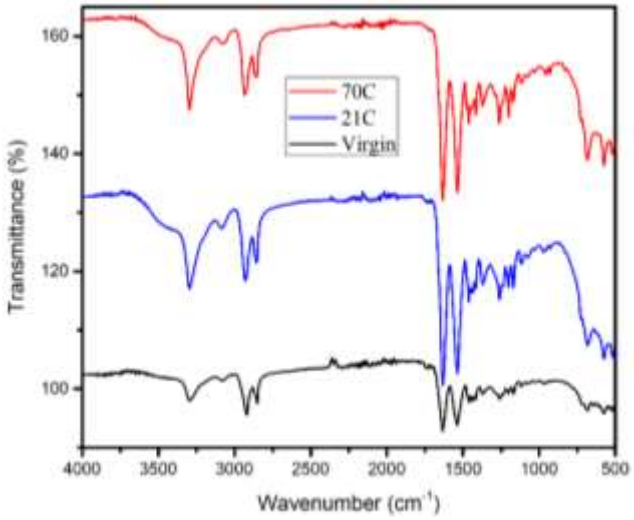

Figure 3. 4 FTIR plot for 3DP Onyx specimen before and after immersion in DI water for 14 days.

3.3.3 IR analysis of IM Nylon

Similar observations are made in IM nylon as with 3D printed nylon, with slight variations in the peaks. It takes a longer period for the water to gradually diffuse and form hydrogen bonds with the nylon's amide groups due to the compact fabrication method of injection molding. The shifts and different peak intensities observed in Figure. 3.5 for 21^{0}C and 70^{0}C show bond scissions to have

occurred in the samples after 14 days immersion in water. Similarly, peaks 1473cm^{-1}, 1461cm^{-1} and 1429cm^{-1} represents CH_2 chain scission bending of the vibrations of the α, γ, α-phases respectively [86]. Just like in the 3DP nylon, longer periods of immersion give room for penetration of moisture in between the polymer chains and similar changes are observed although at lower intensities.

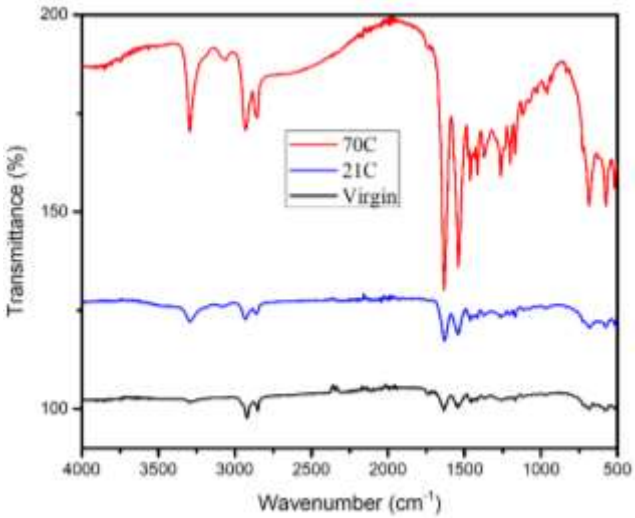

Figure 3. 5 FTIR plot for IM Nylon specimen before and after immersion in DI water for 14 days.

3.3.4 IR analysis of 3D printed Polylactic acid (PLA)

From the FTIR of PLA (Figure 3.6), bands were observed between 3700cm^{-1} and 3000cm^{-1}. These are the stretched -OH groups of the polylactide end units. The other two bands at 2991cm^{-1} and 2943cm^{-1} are the asymmetrical and symmetrical stretching vibrations of CH_3 group. The absorption band at 1753cm^{-1} clearly illustrates the stretching vibrations of the C=O carbonyl group, common with esters, while the peak at 1462cm^{-1} demonstrates asymmetrical deformation vibrations of the CH_3 groups. The two bands at 1235cm^{-1} and 1134cm^{-1} are the symmetrical stretching vibrations of -C-O-C- group. The peaks at 853cm^{-1} and 754cm^{-1} are the stretching of the vibrations of C-COO and deformation vibration of C-O respectively. The O–H band for the virgin 3DP PLA became more pronounced and broader and shifted to slightly lower wave numbers after

14 days immersion in DI. This change can be attributed to the influence of moisture and the free hydroxyl groups that are now engaged in hydrogen bonding [87]. The further increase in intensity and ratio bands at the 1753cm^{-1},1235cm^{-1},1134cm^{-1},853cm^{-1} and 754cm^{-1} after 14 days are possibly due to the hydrolytic degradation to random bond cleavage of the ester bonds as the water had enough time to diffuse and break the ester bonds.

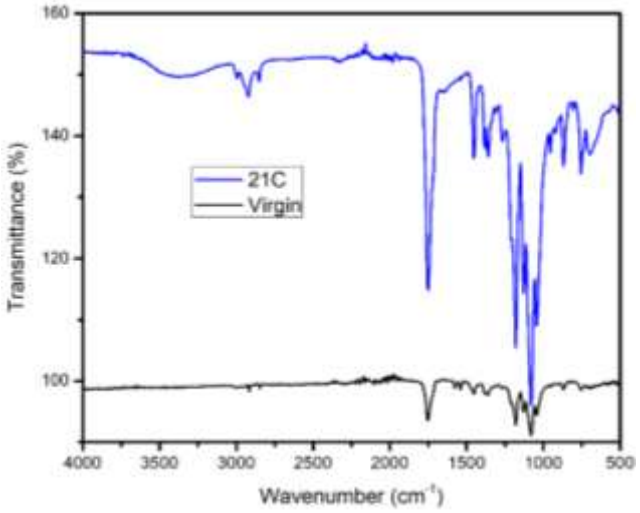

Figure 3. 6 FTIR plot for 3DP PLA specimen before and after immersion in DI water for 14 days.

3.4 Differential Scanning Calorimetry

Differential scanning calorimetry (DSC) is a technique which is used to measure the quantity of heat required to increase the temperature of a sample and its corresponding reference as a function of temperature [88]. In this thermoanalytical technique, the sample and reference are maintained at the same temperature. The DSC results of all the four materials are shown in Figure 3.7 to 3.11. The melting temperature and crystallization temperatures for all four materials are evaluated. A trend is observed in all materials in that after 14 days at 70^{0}C the melting temperature ad crystallization temperatures are reduced when compared to the virgin samples and this was envisaged as the presence of initial heat as a function of the temperature at 70^{0}C was expected to hasten the thermodynamic processes.

3.4.1 3DP Nylon

Nylon absorbs water primarily into its amorphous phase as diffusion into the crystalline phase is very difficult [40]. However, if temperature is continually increased the crystalline phase begins to absorb some moisture because there is more energy available and the intermolecular hydrogen bonds are triggered [82]. As illustrated in Figure 3.7, the crystallization melting point decreases gradually from the virgin nylon to the samples soaked for 14 days at 70^0C. At 21^0C, the materials show very little difference between heating and cooling. It can be postulated that the immersion of the nylon specimens at 21^0C doesn't significantly affect their thermal properties. At 70^0C, however, a reduction is observed in both the heating and cooling which can be attributed to bond breakage, a disruption of the phase due to water diffusion absorption at the elevated temperature, and reorganization of these molecules in the crystalline phase. This reduction is due to the action of hydrogen molecules of the water on the hydrogen bonds adjacent in the nylon chains resulting in the destruction of the nylon crystallinity [38]. Thus, we can confirm that at elevated temperatures, moisture will penetrate into the crystalline parts of the nylon polymer phase and reorganize the phases in the structure degradation.

Table 3. 2 DSC results for 3DP virgin nylon specimen and samples exposed to moisture for 14 days at 21^0C and 70^0C.

Material	Condition	T_g [^{0}C]	T_c [^{0}C]	T_{m1} [^{0}C]	X_c [%]
3DP Nylon	Virgin	48.21	185.00	222.80	14
	21C	54.56	185.06	223.17	24
	70C	52.43	160.51	203.89	10

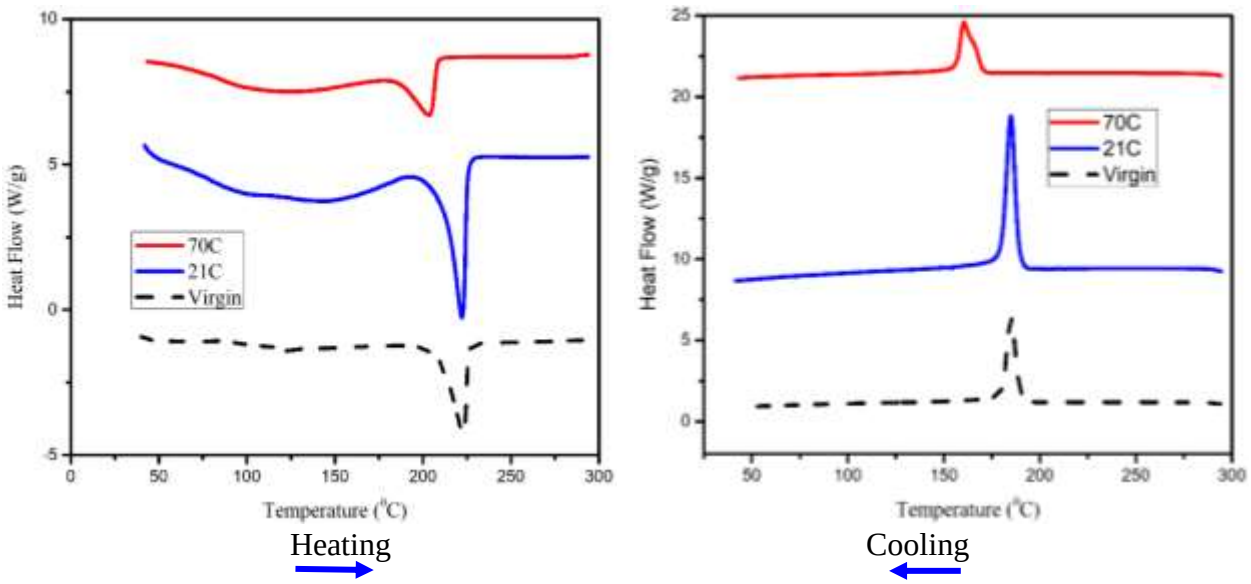

Figure 3. 7 DSC plot for 3DP nylon specimen before and after immersion in DI water for 14 days.

3.4.2 3DP Onyx

The presence of carbon fibers in the Onyx specimens proved to be significant as melting temperature and crystallization temperatures greatly varied compared to its nylon counterpart. Melting and glass transition temperature for the virgin sample was recorded ~200.28^{0}C and ~78.25^{0}C, while the crystallization temperature measured ~162.73^{0}C. This can be largely attributed to the presence of chopped carbon fibers present in the amorphous region of the material serving as reinforcements and reducing chain entanglements in the nylon matrix. Moisture absorbed readily into the 3DP Onyx amorphous phase and carbon molecules are responsible for the faster rate of melting and crystallization after 14 days compared to the plain 3DP and IM nylon samples. Table 3.4 illustrates these results; the crystallization melting point decreases gradually from the virgin nylon to the samples soaked for 14 days at 70^{0}C. At 21^{0}C, the materials show very little difference between heating and cooling. It can be postulated that the immersion of the 3DP Onyx specimens doesn't significantly affect their thermal properties at 21^{0}C but is significant at 70^{0}C.

Table 3. 3 DSC results for 3DP Onyx specimen and samples exposed to moisture for 14 days at 21^0C and 70^0C.

Material	Condition	T_g [^{0}C]	T_c [^{0}C]	T_{m1} [^{0}C]	X_c [%]
3DP Onyx	Virgin	78.25	162.73	200.28	16
	21C	87.85	163.39	200.51	8
	70C	87.73	172.44	201.50	0.1

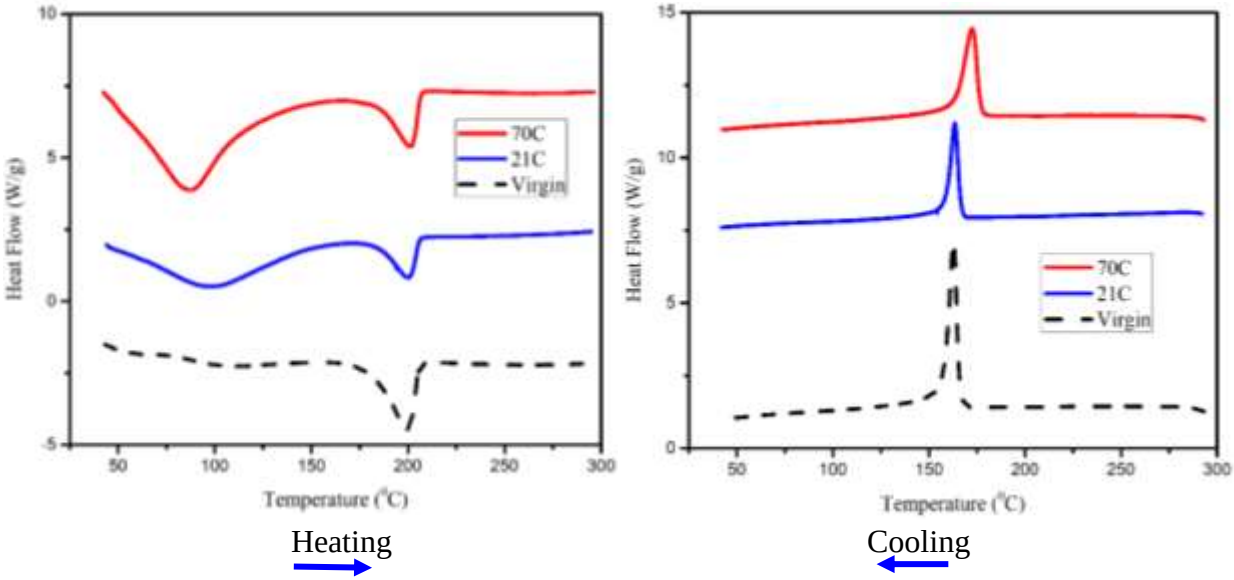

Figure 3. 8 DSC plot for 3DP Onyx specimen before and after immersion in DI water for 14 days

3.4.3 IM Nylon

Observations in IM Nylon were not much different when compared to the 3DP nylon except for the same occurrences happening at slightly different temperatures which can be largely attributed to the changes in material properties. Similarly, the IM nylon sample absorbed moisture via its amorphous phase. Highlighted in Table 3.4, the melting temperature increased after 14 days at 21^0C but decreased insignificantly at 70^0C, while the glass transition temperature also exhibited a similar trend.

Table 3. 4 DSC results for IM nylon specimen and samples exposed to moisture for 14 days at 21^0C and 70^0C.

Material	Condition	T_g [^{0}C]	T_c [^{0}C]	T_{m1} [^{0}C]	X_c [%]
IM Nylon	Virgin	67.70	157.73	200.70	20
	21C	84.41	185.00	221.77	17
	70C	82.95	183.00	221.54	0.3

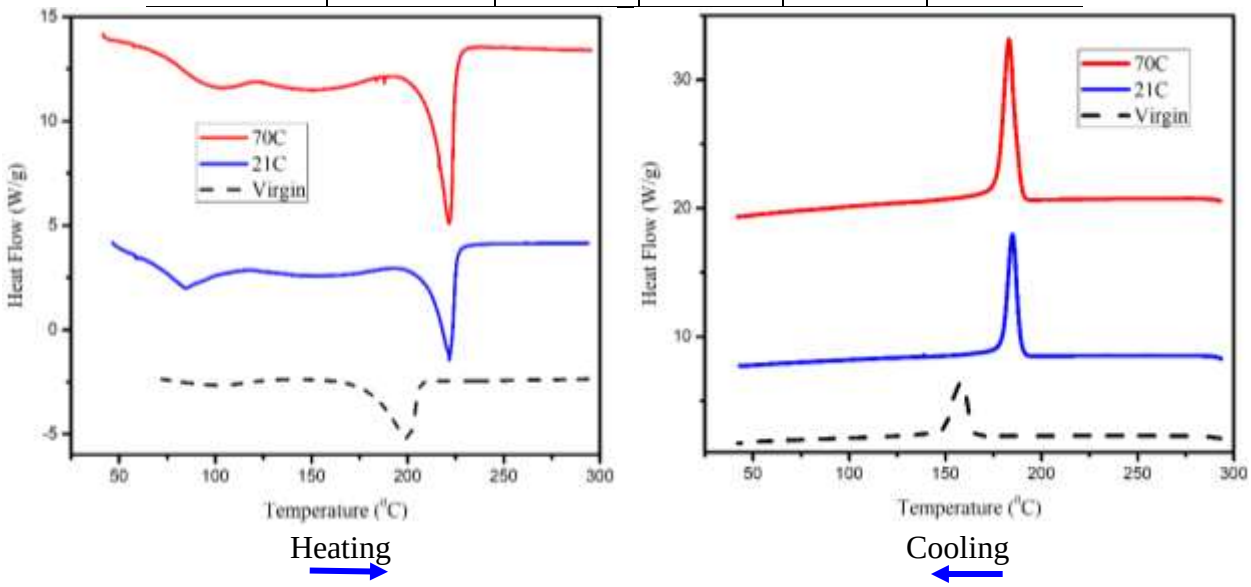

Figure 3. 9 DSC plot for IM virgin nylon specimen before and after immersion in DI water for 14 days.

3.4.4 3DP PLA

The DSC results of the virgin 3DP PLA and PLA after immersion for 14 days are shown in Figure 3.10 below. The melting point and crystallization temperatures are clearly observed in the curves. Notice that there was no glass transition temperature, T_g recorded after 14 days as it is hypothesized that the material was already in its full rubbery region. This can be due to the fact that the moisture caused a breakdown of the physical crosslinks and increased greater mobility of the amorphous fraction in the polymer. The exothermic transition around ~103.69^{0}C in Figure 3.10 is due to the cold crystallization of PLA and further reduces after 14 days. As observed, the melting

temperatures also reduce after 14 days at 70^0C and this may be due to the entanglements in the polymer chains as the specimens are already saturated and desorbing moisture.

Table 3. 5 DSC results for 3DP PLA specimen and samples exposed to moisture for 14 days at 21^0C and 70^0C.

Material	Condition	T_g [^{0}C]	T_c [^{0}C]	T_{m1} [^{0}C]	X_c [%]
3DP PLA	Virgin	57.44	103.69	175.09	41
	21C	-	103.20	173.97	29
	70C	-	95.09	162.49	0.4

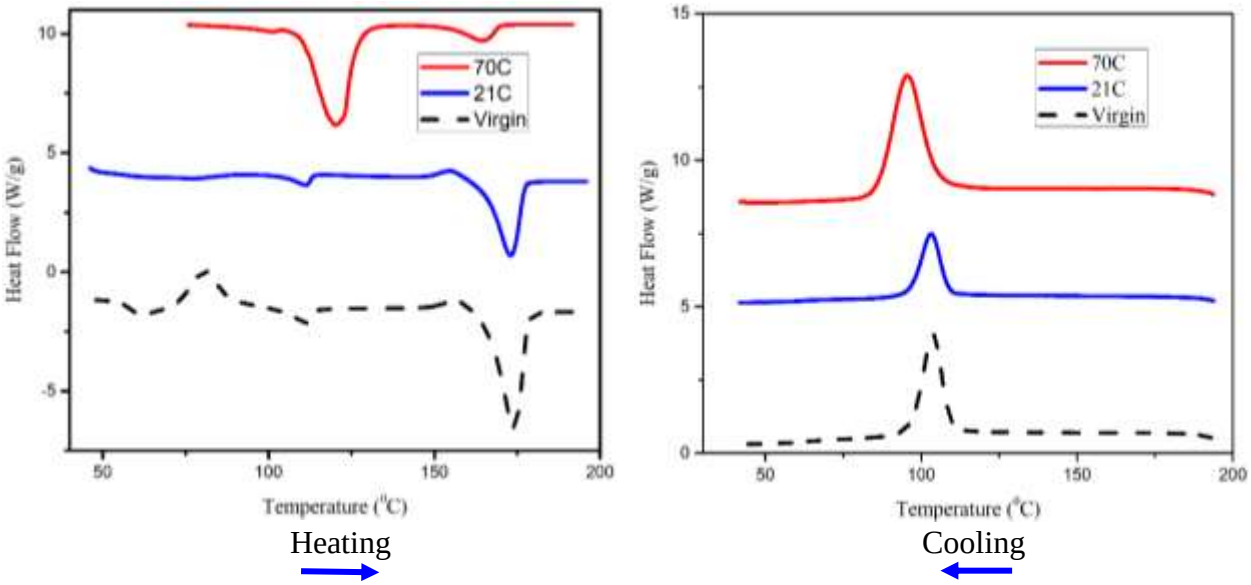

Figure 3.10 DSC plot for 3DP PLA specimen before and after immersion in DI water for 14 days.

4.0 MECHANICAL CHARACTERIZATION

4.1 Flexural Properties

The flexural properties of all four materials were calculated and compared. The results are summarized in Figures 4.1 and 4.2. The flexural properties of the 3DP materials were affected more by moisture absorption compared to the IM nylon. This difference is as result of their method of FDM fabrication in which parts are produced via layers, so the moisture penetrates more easily via the porous spaces between the layers. As a result, their mechanical properties were significantly affected. Plasticization effects and debonding of the molecules when nylon absorbs moisture at longer periods are observed. Higher temperatures (70^0C) increases this effect after just a few days resulting in further decrease in strength and modulus.

A closer observation of the 3DP Onyx samples reveals that although there is a trend in the decrease of flexural strengths and moduli, the absolute values are higher than the nylon specimens. This notable difference in mechanical properties is due to the reinforcement provided by the chopped carbon fibers within the nylon matrix. Also, because plasticization is hindered by the presence of these carbon fillers higher retention of strength and modulus, notably over ~40% greater is observed after 28 days at both temperatures. Meanwhile, for the PLA specimens, the random cleavage of the ester bonds is significantly affected by high temperatures. PLA soaked at 21^0C for 21 days doesn't exhibit large changes in flexural strength and modulus. The minute changes observed can be reversed via drying, proving that bond breakage has not occurred [80]. On the contrary, at 70^0C bond breakage and complete material degradation occurs after only 7 days (~ 61% loss); illustrating that high temperatures play a significant role in the mechanics of PLA polymer degradation.

4.2 Flexural Strength

3DP nylon at 21^0C showed a gradual decrease in flexure strength ~59% after 21 days and an ~44% decrease after 28 days. It is hypothesized that after 21 days the presence of excess moisture changes the material crystallinity of the material making it stronger and thus requiring more force to yield in the flexure testing. However, at 70^0C, this same material exhibited an unexpected pattern in flexural strength over the periods investigated. A ~50% decrease in flexural strength occurred the first 7 days, then finally decreases further in flexural strength by ~44% after 28 days. This undulating pattern at 70^0C can be attributed to elevated temperatures quickening the attainment of moisture equilibrium and desorption and changes in the polymer morphology which is portrayed also at 21^0C but at a slower rate. Thus, it is hypothesized that at longer periods, even nylon at 21^0C will follow such a pattern.

The flexural strength of 3DP Onyx at 21^0C reduced by ~46% within the first 2 days and even further by ~73% after the next 26 days. Meanwhile at 70^0C, a significant reduction of ~66% is observed after 28 days of immersion in DI water.

IM nylon at 21^0C expectedly followed a similar pattern as the 3D printed nylon but with a larger (~90%) decrease in flexural strength observed after 28 days. However, at 70^0C, an increase of ~50% is observed between 1 and 2 days, followed by negligible changes over the next 12 days investigated. Finally, an ~87% decrease after 28 days is observed.

3DP PLA at 21^0C did not exhibit significant changes in flexural strength within the first 14 days. However, a slight increase of ~14% was observed after 28 days. Similarly, virtually no change was measured for the first 2 days at 70^0C. After 7 days at 70C, however, there was a substantial decrease of ~65%. It is important to mention here that the PLA specimens became extremely brittle at this time. Specimens were easily broken by dropping or squeezing them by

hand. The elevated temperature and prolonged immersion, therefore, lead to complete material degradation. This behavior is due to reduced polymer chain entanglements and molecular weight of PLA at elevated temperatures.

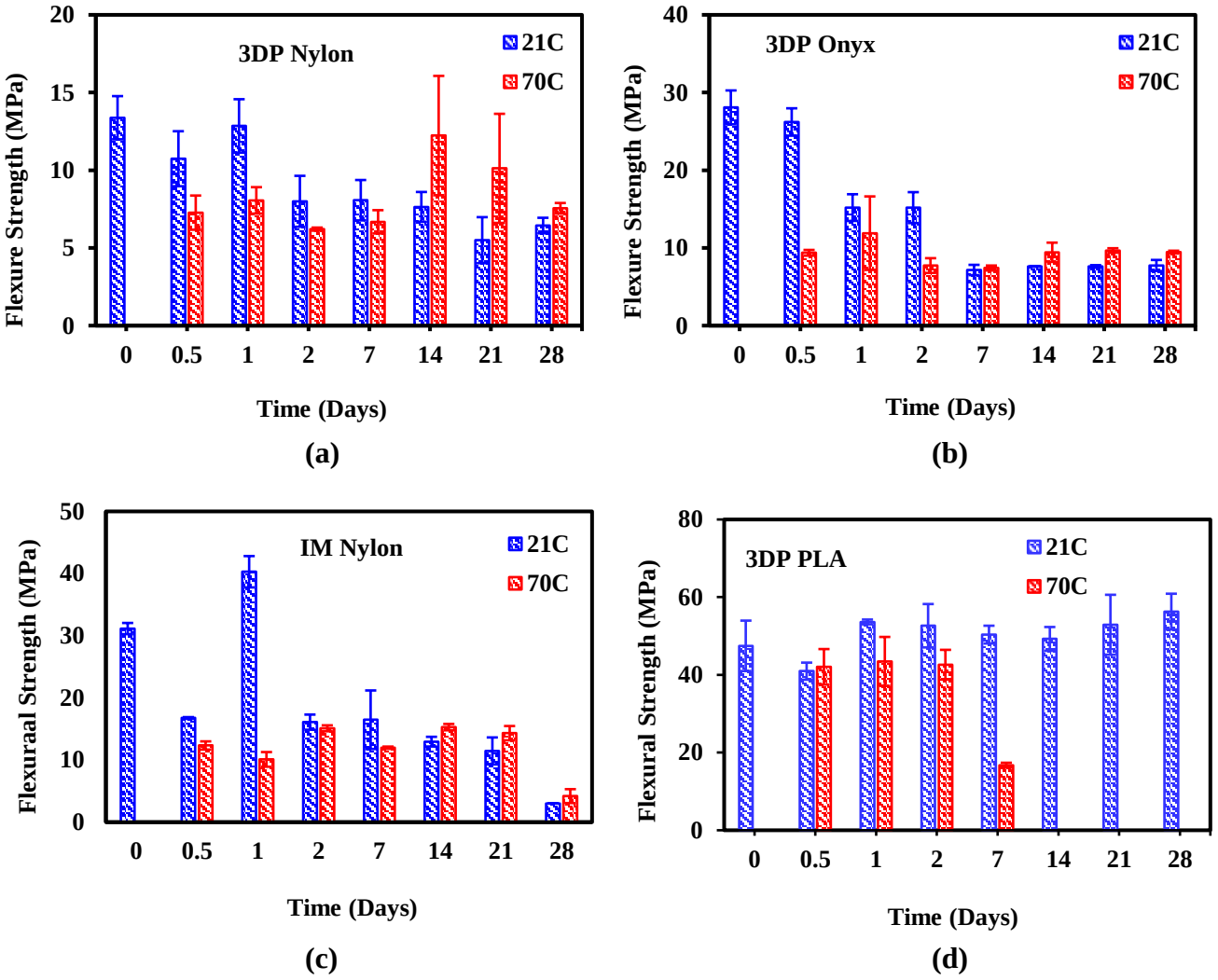

Figure 4. 1 Flexural strength results for all four materials before and after immersion (a) 3DP Nylon (b) 3DP Onyx (c) IM Nylon (d) 3DP PLA

4.3 Flexural Modulus

The flexural modulus is a measure of the bending stiffness of a material. At 21^0C, the modulus of 3DP Nylon decreased by as much as ~67% after 28 days while at 70^0C the decrease in modulus stays relatively constant and then increases ~21% in the period between 7 and 28 days. Overall, reduction in flexural modulus for 3DP Onyx is ~67% after 28 days at 21C and ~57% at 70^0C.

Not much activity is observed for 3DP Onyx and IM Nylon between 1 and 2 days. This indicates that an initially slow process is occurring. However, major changes are observed after 28 days. A ~96.09% is observed in the IM nylon after immersion in DI water at 21^0C for 28 days, and ~92% at 70^0C for this same period. This drastic decrease is attributed to the fact that complete bond breakage /chain scission has occurred after 28 days.

While there was no significant change in the flexural modulus of 3DP PLA in the first 14 days at 21^0C, after 28 days an increase of ~21.19% was observed. The rise in flexural modulus between 14 and 28 days can be attributed to the presence of more water molecules which now serves as a bound residual moisture thus allowing for more energy to be absorbed and thus increased flexural yield strength before eventual failure in the 3DP PLA samples.

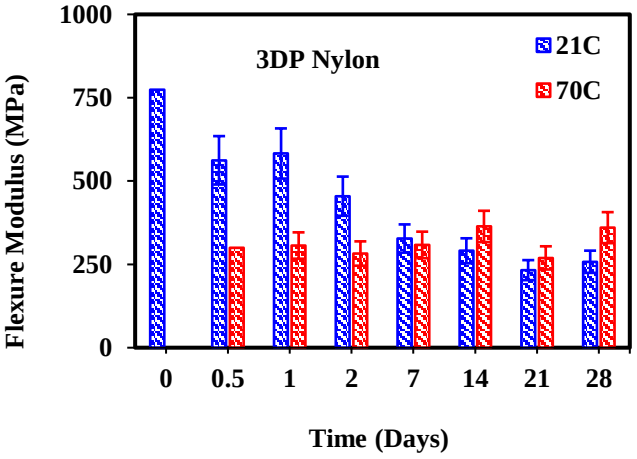

(a)

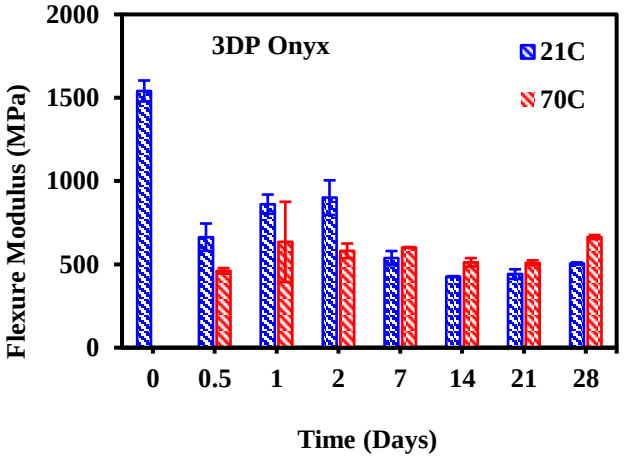

(b)

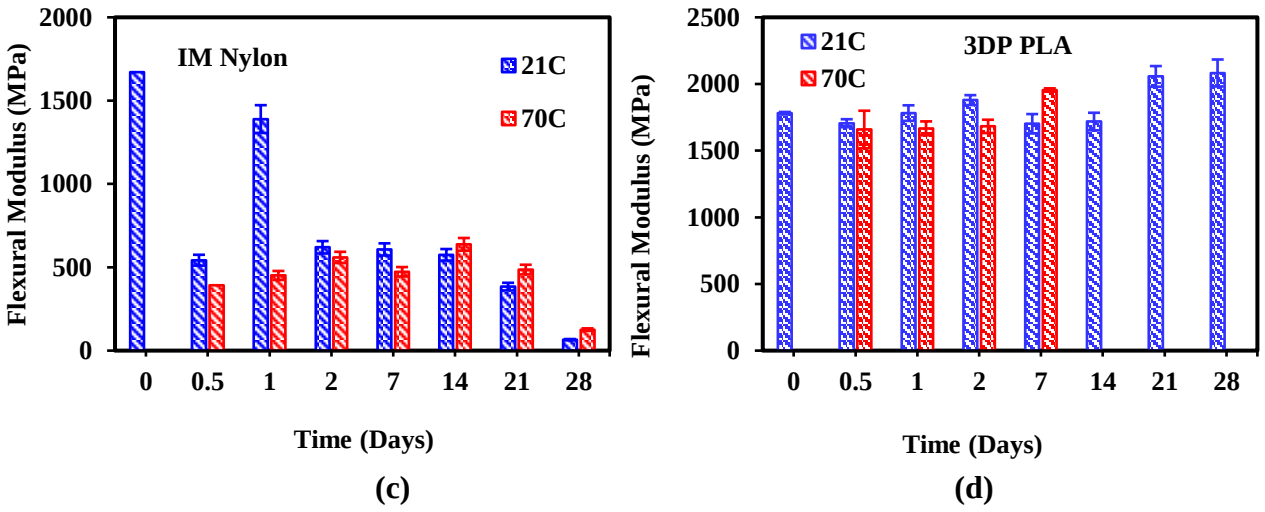

Figure 4. 2 Flexural modulus results for all four materials before and after immersion (a) 3DP Nylon (b) 3DP Onyx (c) IM Nylon (d) 3DP PLA

4.4 3DP Materials at 21^{0}C

The trends in the flexural strength of the 3DP polymer materials at 21^{0}C further reveal the effect of moisture at room temperature and are highlighted in Figure 4.3. As expected 3DP PLA exhibits the highest strength in all the materials evaluated followed by the 3DP Onyx and lastly 3DP Nylon. While ~52% in flexural strength is lost after 28 days in 3DP nylon, 3DP onyx loses as much as 72.45% in its flexural strength. 3DP PLA, however, increases in strength (~19%) after 28 days of immersion. Thus, these results show that after 28 days of immersion of all the 3DP materials, 3DP PLA retains its higher strength, followed by 3DP onyx and 3DP nylon respectively which all can be attributed to the constituent molecular polymer chains. The flexural modulus of 3DP nylon decreases by ~58% after just 7 days of immersion but this rate decreases over the following three weeks. After 7 days, 3DP Onyx at 21^{0}C loses decreases ~65% of its stiffness which then drastically reduces to ~6% of its virgin value for the next 21 days. 3DP PLA had similar

behavioral patterns with its flexural strength with insignificant cases in the early 14 days and little gain 21% gain in flexural modulus for the remaining two weeks.

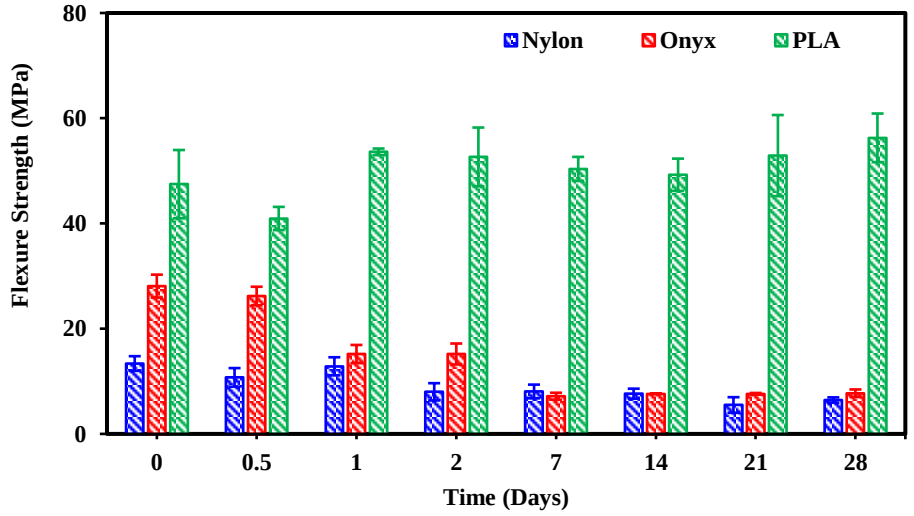

(a)

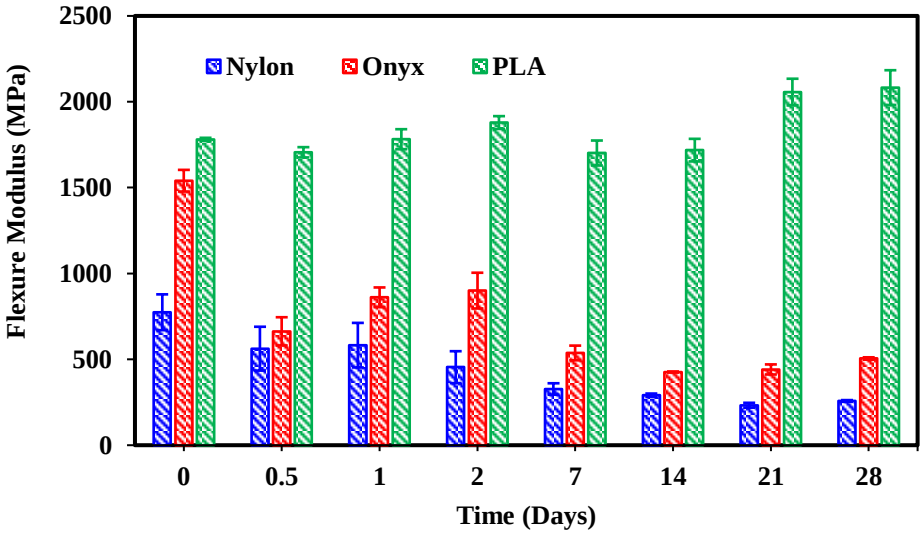

(b)

Figure 4. 3 Flexural properties of 3D printed materials before and after immersion at 21^0C (a) Flexural strength (b) Flexural modulus

4.5 3DP Materials at 70^0C

The influence of high temperatures plays a great role in the absorption and degradation of these materials as they are immersed in DI water. 3DP nylon at 70^0C had a moderate flexural strength up to 7 days but rises ~83% and gradually decreases for the next 14 days down to ~38%.

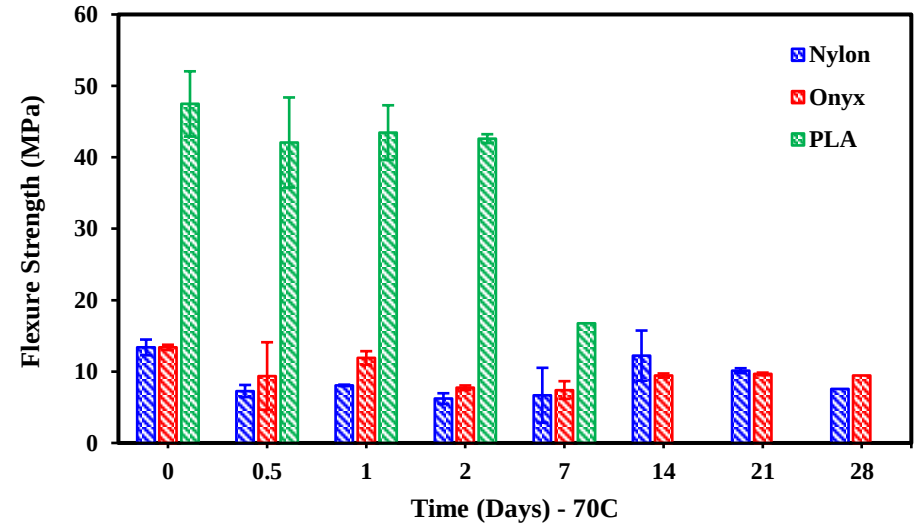

(a)

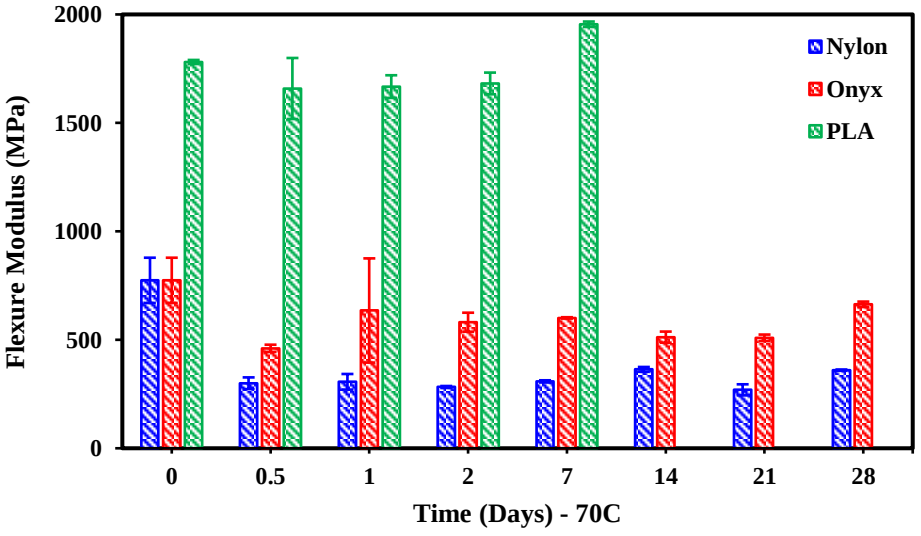

(b)

Figure 4. 4 Flexural properties of 3D printed materials before and after immersion at 70^0C (a) Flexural strength (b) Flexural modulus.

4.6 Stress – Strain behavior

This section takes a closer look at stress - strain behavior of the individual materials from the onset of degradation up to 7 days. As shown in Figure 4.5 and 4.6, all materials exhibit initial linear elastic behavior followed by significant yielding. As expected, the virgin specimens exhibit highest flexural stresses for all 4 materials evaluated. As the materials begin to absorb moisture, however, the maximum stress values and the slopes of the stress versus strain plots decrease appreciably.

It is important to note that after 1 day at 21^0C, there is no significant change in the mechanical behavior of the IM nylon specimens (see Figure 4.6). This result can be attributed to the method of fabrication, injection molding. IM nylon specimens are more compact and stiffer because the samples were prepared at high pressure which is favorable for greater entanglements of the polymer chains, and therefore there is little room for penetration of moisture in the short term. At 70^0C, however, the stress-strain plot after 1 day is similar to that of specimens immersed at 70^0C for 7 days. This is a clear indication that chain scission is more of a function of temperature than time.

As discussed earlier for 3DP PLA, there is very minimal change in the moisture absorption making this material the least hygroscopic of all four in this study. This is reflected in the stress-strain plot where instead of exhibiting suppressed stress-strain plots with immersion time, there is very little difference in the plot and the material actually exhibits a slight increase in yield strength.

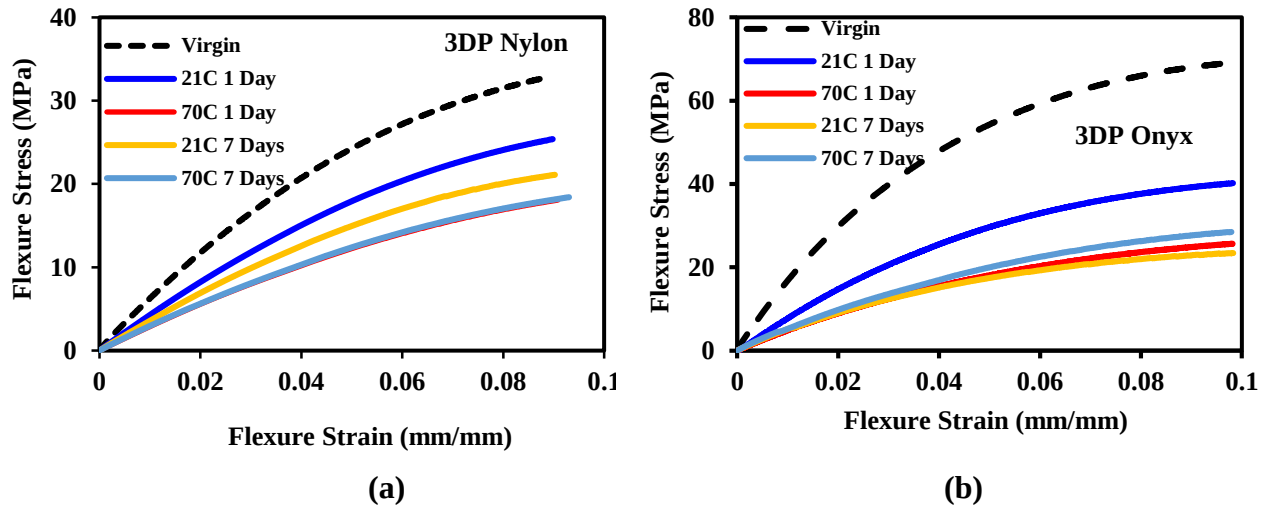

Figure 4. 5 Representative flexure stress versus strain plots after 1 day and 7 days immersion (a) 3DP nylon (b) 3DP Onyx

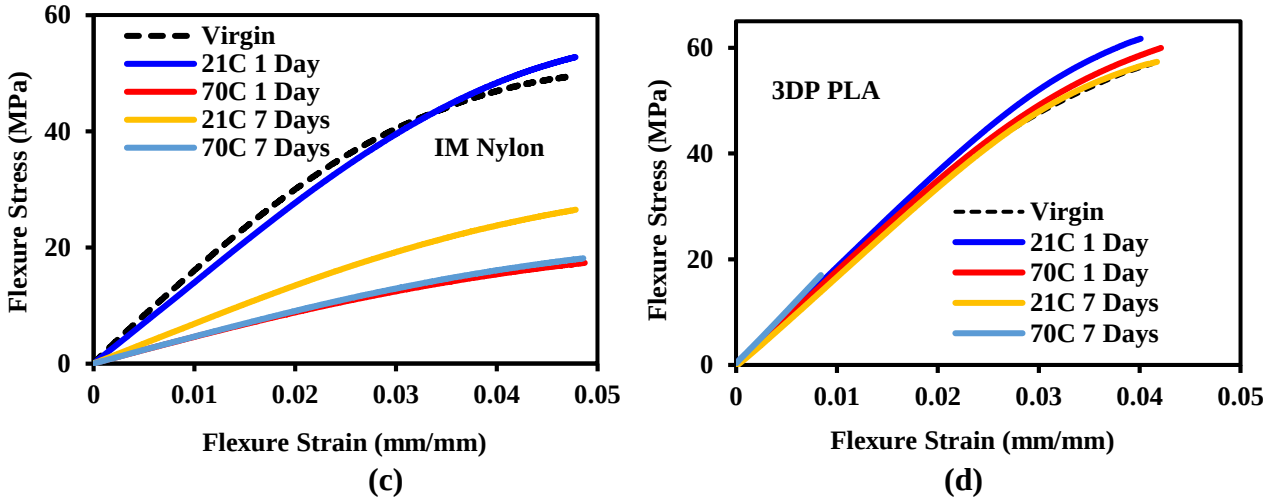

Figure 4. 6 Representative Flexure stress versus strain plot after 1 days and 7 days immersion (C) IM nylon (D) 3DP PLA

5.0 CONCLUSIONS AND FUTURE WORK

5.1 Conclusions

The major objective of this work was to evaluate the moisture absorption mechanisms in 3D printed polymer matrix composites, with the aim of developing materials in the future that can degrade on-demand. The materials investigated in this project were 3D printed nylon, 3D printed PLA, 3D printed polylactic acid (PLA) and injection molded nylon. These materials are hygroscopic and are being actively used in various engineering applications. The moisture absorption behavior of these specimens was evaluated using several tests. Mechanical properties of the specimens were monitored using flexure testing and dynamic mechanical analysis (DMA), while thermal behavior was investigated using differential scanning calorimetry (DSC). Changes in polymer architecture were examined via Fourier transform infrared spectroscopy (FTIR

The following conclusions can be drawn from the results of this research:

3DP nylon is the most hygroscopic of all the four materials evaluated, closely followed by 3DP Onyx, then IM nylon and finally 3DP PLA. The nylon based materials absorbed up to 6% more moisture than the 3DP PLA. Moisture absorption was more prominent in the nylon materials suggesting that the molecular structure was more susceptible to the influence and effects of water molecules. All virgin samples of these materials initially absorbed more moisture than specimens immersed for increased periods of time. This behavior was expected since the virgin samples contained minimal moisture to begin with and should be more amenable to moisture absorption. Moisture absorption rates were higher at initial stages, but slower at elongated periods of immersion. The absorption behavior in these materials can be attributed to the action of both moisture available and temperature.

Exposure to moisture at elevated temperature of 70^0C resulted in higher slopes of the moisture absorption plots in the linear region indicating a faster rate of moisture absorption than samples at 21^0C. This difference can be attributed to the fact that water diffusion is a thermally activated process. At 21^0C, 3DP nylon, 3DP onyx and IM nylon all attained maximum moisture content at ~10%, while 3DP PLA was ~1%. 3DP nylon, 3DP onyx and IM nylon at 70^0C all reached a maximum moisture absorption ~8%, while 3DP PLA attained maximum moisture absorption at ~0.8%. At higher temperature, moisture absorption was rapid but overall concentration lower compared to ambient temperature where the moisture absorption was slower, but more quantity was absorbed.

Results obtained from the DMA tests of the virgin samples were consistent with data in other published work, specifically as regards to glass transition temperature and storage moduli. DSC results revealed the effects of water absorption on the thermal characteristics of all four materials. Virgin samples displayed higher melting and crystallization temperatures. However, samples at both temperatures of 21^0C and 70^0C after 14 days immersion showed decrease in melting and crystallization temperatures indicating that the absorbed moisture caused bond weakening.

FTIR results provided clear illustration of these chain scission reactions occurring, where at specific wave numbers increased intensities of the polymer chains were observed. Specifically, all specimens displayed actions of polymer chain mobility at both temperatures after 14 days in water.

Immersed specimens exhibited reduced strength and stiffness compared to virgin specimens as a result of physical bond weakening and increased polymer chain mobility due to the absorbed moisture. Flexure tests revealed that out of all the materials, 3DP nylon was weakened

more at ambient temperature than 3DP Onyx. For example, after 21 days 3DP nylon at 21^0C retained just ~41% of its flexural strength and ~30% of its flexural modulus, while at 70^0C after 2 days it retained ~47% of its flexural strength. On the other hand, 3DP PLA appeared to maintain its strength and modulus at 21^0C.

5.2 Future Work

The four materials investigated have been extensively characterized via methods such as dynamic mechanical analysis (DMA), Fourier transform infrared spectroscopy (FTIR), differential scanning calorimetry (DSC) and flexure testing. Further testing of nylon, onyx and PLA will also be performed to determine their tensile and fracture properties after immersion in DI water. The results of these investigations will provide a complete overview of the degradation behavior of these materials at ambient temperature and elevated temperature of 70^0C. These results, along with moisture absorption rates, will be used as indices for a numerical model which can predict polymer degradation kinetics and aid in the development of the polymer matrix composites that can degrade on-demand.

REFERENCES

[1] E. H. Backes, L. N. Pires, L. C. Costa, F. R. Passador, L. A. Pessan, 'Analysis of the Degradation During Melt Processing of PLA/Biosilicate® Composites,' Journal of Composite Science (2019) vol. 3, no. 2, p. 52, doi: 10.3390/jcs3020052.

[2] Westport et al., Springer, G. S. (Editor), Environmental Effects on Composite Materials, Technomic, Westport, 1981.

[3] Y. J. Weitsman, M. Elahi, Effects of Fluids on the Deformation, Strength and Durability of Polymeric Composites - An Overview, Mechanics of Time Dependent Materials (2000) 4: 107-126.

[4] Y. J. Weitsman, Effects of Fluids on Polymeric Composites-A Review, Chapter 2.11, Compressive Composite Materials (Kelly, A., Zweben, C., eds.), Elsevier, Oxford (2000) 369-401.

[5] D. Choqueuse, P. Davies, F. Mazeas, R. Baizeau, Aging of Composites in Water: Comparison of Five Materials in Terms of Absorption Kinetics and Evolution of Mechanical Properties, High Temperature and Environmental Effects on Polymer Composites, 2nd Volume, ASTM STP 1302, (1997) 73-96.

[6] Gupta, M.C., Deshmukh, V.G. Thermal oxidative degradation of poly-lactic acid. Colloid & Polymer Science 260 (1982), 308–311. https://doi.org/10.1007/BF01447969.

[7] C. H. Shen, G. S. Springer, Moisture Absorption and Desorption of Composite Materials, Journal of Composite Materials (1976) 10: 2.

[8] D. Hull, T. W. Clyne, An Introduction to Composite Materials, Second Edition, Cambridge University Press, New York, 1996.

[9] G. Marom, L. J. Broutman, Moisture in Epoxy Resin Composites, Journal of Adhesion (1981) 12: 153-164.

[10] C. Williams, Effect of Water Absorption on the Room Temperature Properties of Carbon Fiber and Glass Fiber Reinforced Polymer Composites, Ship Materials Engineering Department, David Taylor Research Center, DTRC/SME-88-85 (1998).

[11] Fincan, Mustafa, "Assessing Viscoelastic Properties of Polydimethylsiloxane (PDMS) Using Loading and Unloading of the Macroscopic Compression Test" (2015). Graduate Theses and Dissertations.

[12] F. R. Jones, Durability of Reinforced Plastics in Liquid Environments, Chapter 3, Reinforced Plastic Durability (Pritchard, G. ed), CRC Press, Boca Raton, (2000).

[13] Y. Diamant, G. Marom, L. J. Broutman, The Effect of Network Structure on Moisture Absorption of Epoxy Resins, Journal of Applied Polymer Science (1981) 26:2015-3025.

[14] F.A. Ramirez, L.A. Carlsson, B.A. Acha, Evaluation of water degradation of vinylester and epoxy matrix composites by single fiber and composite tests Journal of Material Science, 43 (15) (2008), pp. 5230-5242.

[15] D. Suh, M. Ku, J. Nam, B. Kin, S. Yoon, Equilibrium of Water Uptake of Epoxy/Carbon Fiber Composites in Hygrothermal Environmental Conditions, Journal of Composite Materials (2001) 35: 264-278.

[16] Kuda-Malwathumullage, Chamathca Priyanwada. "Applications of near-infrared spectroscopy in temperature modeling of aqueous-based samples and polymer characterization." PhD (Doctor of Philosophy) thesis, University of Iowa (2013), https://doi.org/10.17077/etd.36gsm0e8.

[17] Hosei Shinoda, Krzysztof Matyjaszewski, Structural Control of Poly(Methyl Methacrylate)-g-poly(Lactic Acid) Graft Copolymers by Atom Transfer Radical Polymerization (ATRP), macromolecules (2001) 34, 18, 6243–6248.

[18] Thomas Trimaille, Karine Mondon, Robert Gurny, Michael Möller, Novel Polymeric Micelles for Hydrophobic Drug Delivery Based on Biodegradable Poly(hexyl-Substituted Lactides), International journal of pharmaceuticals (2006) 319(1-2):147-54.

[19] Ogunsona et al., "Accelerated hydrothermal aging of biocarbon reinforced nylon biocomposites, Journal of polymer degradation and stability, (2017) 139: 76-88.

[20] C. F. Baes, R.E. Mesmer, IUPAC. Compendium of Chemical Terminology, 1978.

[21] Z.A.M. Ishak, J.P. Berry, Hygrothermal aging studies of short carbon fiber reinforced nylon 6.6, Journal of Applied Polymer Science (1994), 51.

[22] X. S. Bian, L. Ambrosio, J. M. Kenny, L. Nicolais, A. T. Dibenedetto, Effect of water absorption on the behavior of E-glass fiber/nylon-6 composites, polymer composites (1991), Vol. 12, No. 5.

[23] M. Kohan, Nylon Plastics Handbook, Hanser / Gardner Publications, Inc., New York (1995), 631 pages.

[24] L. Aktas, Y. Hamidi, M. C. Altan, Effect of moisture on the mechanical properties of resin transfer molded composites - Part II: Desorption, Journal of Materials Processing & Manufacturing Science (2002) 10 (4):255–267.

[25] T. Casalini, F. Rossi, A. Castrovinci, G. Perale G, A Perspective on Polylactic Acid-Based Polymers Use for Nanoparticles Synthesis and Applications. Frontiers in Bioengineering and Biotechnology (2019) 7:259. doi: 10.3389/fbioe.2019.00259.

[26] I. Vroman, L. Tighzert, Review: biodegradable polymers, Materials (2009), Vol. 2 No. 2, pp. 307-344.

[27] Campoy, I., Gómez, M. A., & Marco, C. Structure and thermal properties of blends of nylon 6 and a liquid crystal copolyester1Dedicated to the memory of Prof. J.G. Fatou, (1998), Polymer, 39(25), 6279–6288. doi:10.1016/s0032-3861(98)00181-5.

[28] T. Trimaille, K. Mondon, R. Gurny, M. Moller, Novel polymeric micelles for hydrophobic drug delivery based on biodegradable poly (hexyl-substituted lactides), International Journal of Pharmaceutics (2006) 319(1–2):147–54.

[29] B. S. Ndazi, S. Karlsson, Characterization of hydrolytic degradation of polylactic acid/rice hulls composites in water at different temperatures, eXPRESS Polymer Letters, (2011) Vol. 5 No. 2, pp. 119-131.

[30] Yew, G. H., Mohd Yusof, A. M., Mohd Ishak, Z. A., & Ishiaku, U. S. Water absorption and enzymatic degradation of poly(lactic acid)/rice starch composites. Polymer Degradation and Stability, (2005) 90(3), 488–500.

[31] R. M. Taib, S. Ramarad, Z. A. Mohd, M. Todo, Properties of kenaf fiber/polylactic acid biocomposites plasticized with polyethylene glycol, Polymer Composites, (2009) Vol. 31, pp. 1213-1222.

[32] G. W. Melenka, B. K. Cheung, J. S. Schofield, M. R. Dawson, J. P. Carey, Evaluation and prediction of the tensile properties of continuous fiber-reinforced 3D printed structures. Composite Structures (2016) 153:866–75.

[33] L. Li and Q. Sun, Dept. of Mechanical and Manufacturing Engineering C. Bellehumeur, Dept. of Chemical and Petroleum Engineering P. Gu,, Composite Modeling and Analysis for Fabrication

of FDM Prototypes with Locally Controlled Properties, Journal of Manufacturing Processes (2002) Vol. 4/No. 2

[34] P. Parandoush, D. Lin, A review on additive manufacturing of polymer-fiber composites. Composite Structures (2017):182.

[35] X. Wang, M. Jiang, Z. Zhou, J. Gou, D. Hui, 3D printing of polymer matrix composites: a review and prospective. Composites Part B: Engineering (2016) 110:442–58.

[36] T. D. Ngo, A. Kashani, G. Imbalzano, K. T. Nguyen, D. Hui, Additive manufacturing (3D printing): a review of materials, methods, applications and challenges. Composites Part B: Engineering (2018):143.

[37] S. A. Hinchcliffe, K. M. Hess, Experimental and theoretical investigation of prestressed natural fiber-reinforced polylactic acid (PLA) composite materials. Composites Part B: Engineering (2016) 95: 346–54.

[38] R. T.L. Ferreira, I. C. Amatte, T. A. Dutra, D. Bürger, Experimental characterization and micrography of 3D printed PLA and PLA reinforced with short carbon fibers. Composites Part B: Engineering (2017) 124:88–100.

[39] J. Justo, L. Távara, L. García-Guzmán, F. París, Characterization of 3D printed long fibre reinforced composites. Composite Structures (2018):185.

[40] Z. Hou, X. Tian*, J. Zhang, D. Li, 3D printed continuous fibre reinforced composite corrugated structure. Composite Structures (2018):184.

[41] L. E. Murr, Frontiers of 3D printing/additive manufacturing: from human organs to aircraft fabrication. J Mater Sci Technol (2016) 32(10):987–95.

[42] S. Knowlton, B. Yenilmez, S. Tasoglu, Towards single-step biofabrication of organs on a chip via 3D printing. Trends Biotechnology (2016) 34(9):685–8.

[43] S. Ji, M. Guvendiren, Recent advances in bioink design for 3D bioprinting of tissues and organs. Front Bioengineering Biotechnology (2017) 5(23).

[44] E. Lepowsky, S. Tasoglu, 3D printing for drug manufacturing: A perspective on the future of pharmaceuticals. International Journal Bioprint (2018) 4(1).

[45] Kobryn, P.A.; Ontko, N.R.; Perkins, L.P.; Tiley, J.S. Additive Manufacturing of Aerospace Alloys for Aircraft Structures. In Cost Effective Manufacture via Net-Shape Processing, (2006) pp. 3-1 – 3-14. Meeting Proceedings RTO-MP-AVT-139, Paper 3. Neuilly-sur-Seine, France: RTO. Available from: http://www.rto.nato.int/abstracts.asp.

[46] M. R. Talagani, S. Dormohammadi, R. Dutton, C. Godines, H. Baid, F. Abdi F, Numerical simulation of big area additive manufacturing (3D printing) of a full-size car. SAMPE Journal (2015);51(4):27.

[47] N. Labonnote, A. Rønnquist, B. Manum, P. Rüther, Additive construction: state of the art challenges and opportunities. Automation in Construction (2016);72:347–66.

[48] J. I. Lipton, M. Cutler, F. Nigl, C. Dan, H. Lipson, Additive manufacturing for the food industry. Trends Food Science Technology (2015);43(1):114–23.

[49] B. Berman, 3-D printing: the new industrial revolution. Business Horizons (2012) 55:155–62

[50] J. W. Stansbury, J. M. Idacavage, 3D printing with polymers: challenges among expanding options and opportunities, Dental Materials (2016); 34:54–64.

[51] R. Melnikova, A. Ehrmann, K. Finsterbusch, PCM 2014: 2014 global conference on polymer and composite materials; Ningbo, China (2014).

[52] Q. Sun, G. M. Rizvi, C. T. Bellehumeur, P. Gu, Effect of processing conditions on the bonding quality of FDM polymer filaments. Rapid Prototype Journal (2008); 14:72–80.

[53] P. Dudek, FDM 3D printing technology in manufacturing composite elements, Arch. Metall. Mater. 58 (4) (2013) 1415–1418.

[54] T. D. Ngo, A. Kashani, G. Imbalzano, K. T. Q. Nguyen, D. Hui, Additive manufacturing (3D printing): A review of materials, methods, applications and challenges. Composites B (2018); 143:172–96.

[55] N.N. Kumbhar1, A.V. Mulay, Finishing of Fused Deposition Modelling (FDM) Printed Parts by CO2 Laser, Proceedings of 6th International & 27th All India Manufacturing Technology, Design and Research Conference (AIMTDR-2016) College of Engineering, Pune, Maharashtra, INDIA December 16-18, 2016.

[56] https://www.3axis.us/matetials/markforged-materials.pdf

[57] https://www.m-ep.co.jp/en/pdf/product/reny/physicality.pdf

[58] https://www.3dhubs.com/knowledge-base/pla-vs-abs-whats-difference/

[59] ASTM D570-98 (2018), Standard Test Method for Water Absorption of Plastics, ASTM International, West Conshohocken, PA, 2018,

[60] ASTM D4065-12, Standard Practice for Plastics: Dynamic Mechanical Properties: Determination and Report of Procedures, ASTM International, West Conshohocken, PA, 2012.

[61] ASTM D5477-18, Standard Practice for Identification of Polymer Layers or Inclusions by Fourier Transform Infrared Microspectroscopy (FT-IR), ASTM International, West Conshohocken, PA, 2018.

[62] C. Brian, Fundamentals of Fourier Transform Infrared Spectroscopy. 1996.

[63] ASTM D7426-08 (2013), Standard Test Method for Assignment of the DSC Procedure for Determining Tg of a Polymer or an Elastomeric Compound, ASTM International, West Conshohocken, PA, 2013.

[64] Y. Kong, J. N. Hay, The measurement of the crystallinity of polymers by DSC. Polymer (2002); 43, 3873–3878.

[65] B. Wunderlich, The Growth of Crystals. In Macromolecular Physics, 1st ed.; Academic Press: New York, NY, USA, (1976); Volume 3, pp. 115–347.

[66] J. Dong, M. Li, L. Zhou, S. Lee, C. Mei, X. Xu, The influence of grafted cellulose nanofibers and post extrusion annealing treatment on selected properties of poly (lactic acid) filaments for 3D printing. Journal of Polymer Science Part B: Polymer Physics (2017); 55(11): 847–55.

[67] ASTM D7264 / D7264M-15, Standard Test Method for Flexural Properties of Polymer Matrix Composite Materials. ASTM International: West Conshohocken, PA, 2015.

[68] L. Aktas, Y. Hamidi, M. Altan, Effect of moisture on the mechanical properties of resin transfer molded composites - Part I: absorption. Journal of Material Process & Manufacturing Science (2002); 10:239–54.

[69] H. J. Barraza, L. Aktas, Y. K. Hamidi, J. Long, E. A. O'Rear, M. C. Altan, Moisture absorption and wet-adhesion properties of resin transfer molded (RTM) composites containing elastomer-coated glass fibers. Journal of Adhesion Science and Technology (2003); 17:217–42.

[70] H. N. Dhakal, Z. Y. Zhang, M. Richardson, Effect of water absorption on the mechanical properties of hemp fibre reinforced unsaturated polyester composites. Composite Science and Technol0gy (2007); 67:1674–83.

[71] A. R. Berens, H. B. Hopfenberg, Diffusion and relaxation in glassy polymer powders: 2. Separation of diffusion and relaxation parameters. Polymer (1978); 19:489–96.

[72] P. M. Jacobs, E. R. Jones, Diffusion of moisture into two-phase polymers - Part 2 Styrenated polyester resins. Journal of Material Science (1989); 24:2343–7.

[73] S. Roy, W. X. Xu, S. J. Park, K. M. Liechti, Anomalous moisture diffusion in viscoelastic polymers: modeling and testing. Journal of Applied Mechanics (2000); 67:391.

[74] H. G. Carter, K. G. Kibler, Langmuir-type model for anomalous moisture diffusion in composite resins. Journal of Composite Materials (1978); 12:118–31.

[75] G. E. Guloglu, Y. K. Hamidi, M. C. Altan, Fast recovery of non-fickian moisture absorption parameters for polymers and polymer composites. Polymer Engineering Science (2016); 57:921–31.

[76] A. Regazzi, R. Léger, S. Corn, P. Ienny, Modeling of hydrothermal aging of short flax fiber reinforced composites. Composite of Applied Science Manufacturing (2016); 90:559–66.

[77] T. Peret, A. Clement, S. Freour, F. Jacquemin. Numerical transient hygro-elastic analyses of reinforced Fickian and non-Fickian polymers. Composite Structures (2014); 116:395–403.

[78] https://en.wikipedia.org/wiki/Dynamic_mechanical_analysis

[79] P. Adriaensens, Quantitative magnetic resonance imaging study of water uptake by polyamide 4,6, Polymer 42 (2001); 7943e7952.

[80] C. García-Pérez1, C. Menchaca-Campos, M. A. García-Sánchez, E. Pereyra-Laguna, O. Rodríguez-Pérez, Uruchurtu-Chavarín, Journal (2017) Nylon/Por- phyrin/Graphene Oxide Fiber Ternary Composite, Synthesis and Characterization. Open Journal of Composite Materials, 7, 146-165.

[81] B. Frank, P. Frübing, P. Pissis, Water sorption and thermally stimulated depolarization currents in nylon-6, Journal of Polymer Science Physics 34 (1996).

[82] E. Laredo, M.C. Hernandez, Moisture effect on the low- and high-temperature dielectric relaxations in nylon-6, Journal of Polymer Science Part B: Polymer Physics 35 (1997).

[83] R.M. Neagu, E. Neagu, A. Kyritsis, P. Pissis, Dielectric studies of dipolar relaxation processes in nylon 11, Journal of Physics D: Applied Physics, (2000) Volume 33, Issue 15, pp. 1921-1931.

[84] F. Navarro-Pardo, G. Martínez-Barrera, A. Martínez-Hernández, V. Castaño, J. Rivera-Armenta, F. Medellín-Rodríguez, Effects on the Thermo-Mechanical and Crystallinity Properties of Nylon 6,6 Electrospun Fibres Reinforced with One Dimensional (1D) and Two-Dimensional (2D) Carbon. Materials (2013); 6:3494–513

[85] S. Wong, R. Shanks, A. Hodzic, Interfacial improvements in poly(3-hydroxybutyrate)-flax fibre composites with hydrogen bonding additives. Compos Sci Technol (2004); 64: 1321–1330.

[86] https://en.wikipedia.org/wiki/Differential_scanning_calorimetry.